学位論文

Study of the tethering complexes acting on vacuolar trafficking pathways of *Arabidopsis thaliana*

(シロイヌナズナを用いた液胞輸送経路ではたらく繋留複合体の研究**)**

平成 **29** 年 **12** 月　博士（理学）申請

東京大学大学院理学系研究科

生物科学専攻

竹元　廣大

Abstract

Membrane trafficking plays pivotal roles in various cellular activities and higher-order functions of eukaryotes and requires tethering factors to mediate contact between transport intermediates and target membranes. Two evolutionarily conserved tethering complexes, CORVET (class C core vacuole/endosome tethering) and HOPS (homotypic fusion and protein sorting), are known to act in endosomal/vacuolar transport in yeast and animals. These complexes share a core subcomplex consisting of Vps11, Vps18, Vps16, and Vps33, and in addition to this core, HOPS contains Vps39 and Vps41, whereas CORVET contains Vps3 and Vps8. CORVET and HOPS subunits are also conserved in the model plant *Arabidopsis thaliana*. However, vacuolar trafficking in plants occurs through multiple unique transport pathways, and how these conserved tethering complexes mediate endosomal/vacuolar transport in plants has remained elusive. In this study, I investigated the functions of VPS18, VPS3, and VPS39, which are core complex, CORVET-specific, and HOPS-specific subunits, respectively. Biochemical and microscopic analyses revealed that CORVET acts with canonical RAB5, whereas HOPS acts with RAB7. Impairment of these tethering proteins resulted in embryonic lethality and perturbing transport of a vacuolar membrane protein. The CORVET subunits colocalized and interacted with a plant specific R-SNARE, VAMP727, which mediates fusion between endosomes and the vacuole, whereas the HOPS subunits colocalized and interacted with another R-SNARE, VAMP713, which likely mediates homotypic vacuolar fusion. These results indicate that CORVET and HOPS act in distinct vacuolar trafficking pathways in plant cells, unlike those of non-plant systems that involve sequential action of these tethering complexes during vacuolar/lysosomal trafficking. These results highlight a unique diversification of vacuolar/lysosomal transport that arose during plant

evolution, utilizing evolutionarily conserved tethering components.

Table of contents

Acknowledgements

First of all, I would like to express my sincerest appreciation to my two supervisors Professor Akihiko Nakano and Professor Takashi Ueda, for giving me the opportunity to do my dissertation work in their laboratories and for supervising and encouraging me throughout the course of this study.

I thank Professor Miyo Terao Morita (Nagoya University, Japan), Professor Shoji Mano (NIBB, Japan), Professor Taku Demura (NAIST, Japan), Dr. Emi Ito (ICU, Japan), and Professor Tsuyoshi Nakagawa (Shimane University, Japan) for sharing materials, as well as the ABRC and the Salk Institute for providing Arabidopsis mutants.

Technical support was provided by the Functional Genomics Facility, NIBB Core Research Facilities, and the Model Plant Research Facility, NIBB BioResource Center.

I would like to thank all members of Laboratory of Developmental Cell Biology, University of Tokyo, and Division of Cellular Dynamics, National Institute for Basic Biology for their discussions and supports. I thank Professor Karin Schmacher (Heidelberg University, Germany), Dr. Falco Krüger, Dr. Tomohiro Uemura, Dr. Tatsuaki Goh, Dr. Kazuo Ebine, Dr. Takeshi Inoue, and Ms. Jana Christin Askani for their kind advices and discussions.

Last but not least, I would like to express my special thanks to my family for their mental supports and encouragements throughout the years.

Chapter 1: Introduction

Plant vacuoles have diverse and specialized functions including storage of numerous materials, osmo-regulation, recycling and degradation of cellular components, coloring flowers and fruits, and filling space for cell elongation (Zhang *et al*., 2014). In association with these complex functions, plants have evolved their unique vacuolar trafficking mechanisms. For example, *de novo*-synthesized vacuolar proteins are transported to the vacuole via multiple transport pathways, which are regulated by systems distinct from mammalian and yeast lysosomal/vacuolar trafficking pathways (Ebine *et al*., 2014). The majority of newly synthesized vacuolar proteins are transported through the *trans*-Golgi network (TGN). In plants, the TGN also functions as the early endosome in endocytosis (Viotti *et al*., 2010), which further highlights the unique organization of endocytic/vacuolar traffic in plant cells.

Regardless of the unique diversification of the plant vacuolar/endocytic transport system, the majority of transport components are shared between plants and non-plant systems. Rab GTPase is a key regulator for targeting and docking of transport intermediates, such as membrane vesicles, to target membranes, and promoting assembly of tethering complexes that mediate attachment of specific transport vesicles/organelles to their destination membranes. Soluble NSF attachment protein receptor (SNARE) is another key component of the membrane trafficking machinery. SNARE proteins form complexes on the tethered membranes and promote membrane fusion (Figure 1). RAB5 and RAB7 are evolutionarily conserved subgroups of Rab GTPase, which in animal systems act in early and late endosomal trafficking, respectively. While these subgroups are conserved in plants and act in endosomal/vacuolar trafficking, their functions seem to have diverged from those of their orthologs in animals. For example, plant RAB5 mainly

resides on multivesiculated late endosomes rather than on early endosomes (Haas et al., 2007). Some vacuolar membrane proteins are transported through a RAB5-dependent, RAB7-independent pathway (Ebine *et al*., 2014), whereas a similar transport pathway has not been identified in mammals. Conversely, in mammalian cells, RAB5 mediates homotypic fusion between early endosomes, although homotypic early endosomal/TGN fusion has not been described in plant cells. In addition to canonical RAB5, plants are also equipped with a plant-specific RAB5 variant, the ARA6 group, which is another peculiarity specific to plant endosomal transport (Ebine *et al*., 2011). Unlike canonical RAB5, which is isoprenylated at the C-terminus, ARA6 is fatty-acylated at the N-terminus, and it seemingly acts in a counteracting fashion to RAB (Ueda et al., 2001). The genome of *A. thaliana* harbors three RAB5 members: two canonical RAB5 genes, *ARA7*/*RABF2b* and *RHA1*/*RABF2a*, and plant specific *ARA6*/*RABF1* (Anuntalabhochai *et al*., 1991; Ueda *et al*., 2001). SNARE proteins are divided into two categories, R- and Q-SNAREs, depending on the amino acid at the 0-layer in the helical SNARE domain. Q-SNAREs are further divided into Qa-, Qb-, Qc, and Qb+c-SNAREs according to sequence similarity (Wickner and Schekman, 2008). One R-SNARE and three Q-SNAREs, one from each of the Q-SNARE subgroups (or two Q-SNAREs in the case of Qa- with Qb+c-SNARE), assemble into a tight complex, leading to fusion between R-SNARE-bearing and Q-SNARE-containing membranes (Wickner and Schekman, 2008). Two distinct vacuolar SNARE complexes have been identified in *Arabidopsis thaliana*; one complex consists of Qa-SYP22, Qb-VTI11, Qc-SYP5, and R-VAMP71, and the other contains R-VAMP727 instead of VAMP71 (Ebine *et al*., 2011; Fujiwara *et al*., 2014). VAMP727, which is unique to the plant lineage, harbors a characteristic insertion in its N-terminal longin domain. VAMP727 has been shown to mediate membrane fusion

between multivesicular endosomes and the vacuole (Ebine *et al*., 2008), although whether the two vacuolar SNARE complexes are functionally different and how they are regulated during vacuolar transport remain unknown.

Endosomal/vacuolar RAB GTPases and SNARE complexes are functionally connected by tethering complexes, which interact with both RAB GTPases and SNARE proteins to mediate tethering of two membranes before membrane fusion (Wickner and Schekman, 2008). In yeast, two hexameric tethering complexes, CORVET and HOPS, have been shown to mediate transport from the endosome to the vacuole (Peplowska *et al*., 2007; Seals *et al*., 2000). Both complexes share a core subcomplex composed of Vps11, Vps16, Vps18, and Vps33 (Nickerson *et al*., 2009), and in addition, HOPS contains Vps39 and Vps41 (Seals *et al*., 2000), while CORVET contains Vps3 and Vps8 (Peplowska *et al*., 2007). HOPS interacts with RAB7-like Ypt7 and vacuolar SNARE proteins including Vam3, a homolog of plant SYP22 (Seals *et al*., 2000), to mediate membrane fusion between late endosomes and vacuole and controls homotypic fusion of vacuolar membranes (Balderhaar and Ungermann, 2013; Cabrera *et al*., 2010; Ostrowicz *et al*., 2010). Conversely, CORVET binds to RAB5-like Vps21 and mediates tethering of Vps21-positive endosomes (Cabrera *et al*., 2013). The functions of CORVET and HOPS complexes are largely conserved in mammalian cells as well (Caplan *et al*., 2001; Huizing *et al*., 2001; Lachmann *et al*., 2014; Perini *et al*., 2014; Pols *et al*., 2013).

In Arabidopsis, homologs for all subunits of the CORVET and HOPS complexes are conserved (Klinger *et al*., 2013; Vukaġinoviĺ and Ģárský, 2016), some of which play essential roles in embryogenesis and/or gametophyte functions. The Arabidopsis *vacuoless1 (vcl1)* mutant, which harbors a mutation in the *VPS16* gene, exhibits severe defects in vacuole biogenesis (Rojo *et al*., 2001). Recently, *VPS11* and *VPS41* were also

reported to be required for vacuole biogenesis during embryogenesis and pollen tube growth (Hao *et al*., 2016; Tan *et al*., 2017). In contrast, functions of CORVET-specific subunits in endosomal/vacuolar trafficking have not yet been explored in plants, and the functional linkages between RAB GTPases, tethering complexes, and SNARE complexes involved in endosomal/vacuolar transport remain totally unknown. To elucidate how these evolutionarily conserved components fulfill their functions in the uniquely developed plant endosomal/vacuolar transport system, I conducted comparative analyses of VPS18, VPS3, and VPS39, which represent core complex, CORVET-specific, and HOPS-specific subunits, respectively. I found that CORVET and HOPS specifically interact with canonical RAB5 and RAB7, respectively, and act in separate vacuolar trafficking pathways involving distinct sets of SNARE proteins. These results provide further evidence that plants have evolved unique endosomal/vacuolar trafficking pathways, which has been achieved by coordinating evolutionarily conserved components with unique plant-specific machinery.

Chapter 2: Results

CORVET and HOPS complexes in *A. thaliana*

The genome of *A. thaliana* contains homologs of all subunits for the CORVET and HOPS complexes (Klinger *et al*., 2013; Vukaĝinoviĺ and Ţárský, 2016). Although formation of the core complex by VPS11, VCL1/VPS16, and VPS33 has been reported (Rojo *et al*., 2003), it is still unclear whether subunits specific to CORVET and HOPS also assemble into their respective complexes in plants. To examine protein-protein interactions of CORVET- and HOPS-specific subunits with the core complex, I performed yeast two-hybrid assays using DNA binding domain (BD)-fused VPS11 and activation domain (AD)-fused VPS3 or VPS39. VPS11 interacted with both VPS3 and VPS39 in yeast (Figure 2). I then investigated whether CORVET and HOPS complexes form *in planta*. Monomeric green fluorescent protein (mGFP)-tagged VPS18 was expressed in Arabidopsis and immunoprecipitated using an anti-GFP antibody, and interacting proteins were analyzed by mass spectrometry. I detected all subunits of CORVET and HOPS except for VPS8 in the precipitate, whereas free GFP did not precipitate any subunits of these complexes (Figure 3). These results indicate that CORVET and HOPS complexes exist in Arabidopsis cells.

Subcellular localization of CORVET and HOPS subunits

To examine the subcellular localization of CORVET and HOPS, I expressed mGFP-VPS18, mGFP-VPS3, and VPS39-mGFP in *vps18*, *vps3*, and *vps39* mutants, respectively, under control of their native promoters. These chimeric proteins rescued the lethality of the corresponding mutants (described below), which indicated the functionality of these chimeric proteins (Figure 4). Confocal microscopy revealed that mGFP-VPS18 localized to subdomains of the vacuolar membrane and punctate compartments in the cytoplasm,

with faintly dispersed distribution in the cytosol. mGFP-VPS3 was primarily targeted to cytoplasmic punctate structures with no detectable vacuolar membrane localization, whereas VPS39-mGFP was mainly observed on subdomains of the vacuolar membrane with a small number of punctate structures in the cytoplasm (Figure 5). I then coexpressed VPS18 with either VPS3 or VPS39 tagged with distinct fluorescent proteins, which revealed that VPS3 colocalized with VPS18 on cytoplasmic puncta, while VPS39 mainly colocalized with VPS18 on subdomains of the vacuolar membrane (Figure 6). Staining with FM4-64 also indicated that mGFP-VPS18 and VPS39-mGFP were sometimes observed at the vertex zone, the ring-shaped edge of vacuole-vacuole contact sites (Figure 7).

CORVET and HOPS interact with distinct RAB GTPases

In yeast, CORVET and HOPS are known to interact with Vps21/RAB5 and Ypt7/RAB7, respectively, acting as effectors. I examined whether this holds true in Arabidopsis by performing co-immunoprecipitation with the lysate prepared from transgenic plants expressing mGFP-VPS3 or VPS39-mGFP. When using an anti-GFP antibody, mGFP-VPS3 co-precipitated with canonical RAB5 (ARA7 and RHA1) but not with RAB7, whereas VPS39 co-precipitated with RAB7 but not with RAB5 (Figure 8). Thus, specific interactions between endosomal/vacuolar tethers and the Rab GTPases are conserved in plants. In addition to conventional *RAB5*, Arabidopsis has plant specific *RAB5*, *ARA6*. To clarify the relationship between CORVET and the two types of plant RAB5, I performed a Y2H assay using AD-VPS3 and BD-RAB5s. As shown in Figure 9, VPS3 interacted with WT and GTP-fixed form of canonical ARA7, but not with plant-specific ARA6. This result suggests that CORVET acts with canonical RAB5 but not with ARA6.

To further verify these interactions, I compared the subcellular localization of CORVET and HOPS with ARA7 and a RAB7 member, RABG3f, which primarily localize to multivesicular endosomes and the vacuolar membrane, respectively (Ebine *et al*., 2011; Ebine *et al*., 2014) . mRFP-ARA7 exhibited strong colocalization with mGFP-VPS3 in cytoplasmic puncta, but not with VPS39-mGFP (Figure 10). Conversely, Venus-RABG3f exhibited only partial colocalization with mGFP-VPS3 at cytoplasmic punctate structures, although colocalization at subdomains of the vacuolar membrane was observed with VPS39-mGFP (Figure 11). Consistent with the hypothesis that VPS18 is a subunit of the core complex shared between CORVET and HOPS, mGFP-VPS18 exhibited colocalization with mRFP-ARA7 and Venus-RABG3f (Figure 10, 11). I also noticed that VPS39 and RABG3f frequently colocalized at contact sites between two vacuoles. These results strongly suggest that CORVET acts with canonical RAB5 on multivesiculated endosomes, whereas HOPS and RAB7 coordinate the tethering between homotypic vacuolar membranes.

To further investigate the relationship between the tethering complexes and Rab GTPases, I next examined the effects of compromised Rab activation on the subcellular localization of subunits of the two tethering complexes. For this purpose, I expressed mGFP-tagged VPS18, VPS3, and VPS39 in the *vps9a-2* and *ccz1a ccz1b* (hereafter indicated as *ccz1ab*) backgrounds, which are mutants of nucleotide exchange factors for RAB5 and RAB7, respectively (Ebine *et al*., 2014; Goh *et al*., 2007). In *vps9a-2*, mGFP-VPS3 was dispersed through the cytosol with residual localization to punctate cytoplasmic structures, suggesting that RAB5 activation is required for efficient localization of VPS3 to RAB5-positive endosomes. Intriguingly, mGFP-VPS18 and VPS39-mGFP were still localized to the vacuolar membrane in *vps9a-2*, though their

distribution was more uniform than in wild-type plants (Figure 12). On the other hands, in *ccz1ab*, membrane attachment of VPS39-mGFP was hardly detected, while mGFP-VPS3 was still localized to punctate structures, some of which were dilated similarly to RAB5-positive endosomes previously observed in *ccz1ab* (Figure 13, (Ebine *et al.*, 2014)). Localization of mGFP-VPS18 to the vacuolar membrane was also barely detected, though its endosomal localization, which was partially expanded, was retained in this mutant. Taken together, CORVET requires RAB5 activation for endosomal localization, whereas localization of HOPS on the vacuolar membrane depends on RAB7 activation.

CORVET and HOPS are required for normal development of Arabidopsis

I then investigated the significance of CORVET and HOPS in plant development. I examined phenotypes of *vps18*, *vps3*, and *vps39* T-DNA insertion mutants, illustrated in Figure 14. PCR-based genotyping of the progeny from self-pollinated heterozygous mutant plants revealed that homozygous mutants were inviable for all of three genes, and the segregation ratios of the wild-type to heterozygous mutant plants were between 1:1 and 1:2 ($VPS18^{+/+}$:$VPS18^{+/}$ = 96:140, $VPS3^{+/+}$:$VPS3^{+/-}$ = 105:144, and $VPS39^{+/+}$:$VPS39^{+/-}$ = 59:105), suggesting that the homozygous mutations resulted in embryonic lethality. Consistently for all three genes, yellowish seeds were observed in siliques of heterozygous plants (Figure 15), in which developmentally retarded or abnormally shaped embryos were observed (Figure 16). To investigate whether the mutations also affected gametophyte functions, I carried out a reciprocal crossing analysis. Each mutation was heritable via female gametophytes at slightly lower efficiency, but transmission of the mutations from male gametophytes was markedly affected (Table 1). Thus, the functions of CORVET and HOPS are required for normal gametophyte function and embryogenesis in Arabidopsis.

Distinct requirements for CORVET and HOPS in vacuolar transport

Vacuolar transport in Arabidopsis occurs through multiple transport pathways, with distinct functions for RAB5 and RAB7 (Ebine *et al*., 2014). Among these pathways, SYP22 is transported through a RAB5-dependent, RAB7-independent pathway in root epidermis cells. I further investigated requirement for CORVET and HOPS in this trafficking pathway by expressing mRFP-SYP22 in *vsp18*, *vps3*, and *vps39* embryos. In WT-like embryos from siliques of heterozygous mutants, mRFP-SYP22 localized to the vacuolar membrane (Figure 17), as observed in other tissues (Sato *et al*., 1997). In contrast, mRFP-SYP22 was mistargeted to the plasma membrane in homozygous mutant embryos of *vps3* (Figure 18), reminiscent of SYP22 mislocalization to the plasma membrane in root epidermal cells of the *vps9a-2* mutant (Ebine *et al*., 2014). Intriguingly, in the *vps39* mutant embryo, mRFP-SYP22 localized to punctate structures, probably fragmented vacuoles, without localization to the plasma membrane (Figure 17). The mistargeting of SYP22 to the plasma membrane in the *vps3* mutant was not due to an absence of the vacuole in this mutant embryo, because GFP-VAMP713, which is transported to the vacuolar membrane through a distinct trafficking pathway involving the adaptor protein complex-3 (AP-3) (Ebine *et al*., 2014), localized to the vacuolar membrane when coexpressed with mRFP-SYP22 in the *vps3* mutant (Figure 18). These results indicate that CORVET is required for vacuolar transport of SYP22, although it is dispensable for central vacuole formation.

CORVET and HOPS act with distinct SNARE complexes

As described above, impairments in CORVET and HOPS conferred distinct effects on vacuolar morphology and transport, which strongly suggests that these tethering

complexes act in different vacuolar transport events. Given the reported interaction between the CORVET and HOPS core complex with SYP22 in Arabidopsis (Rojo *et al*., 2003), the distinct functions of CORVET and HOPS may be the result of distinct interactions with two SYP22-containing vacuolar SNARE complexes utilizing different R-SNAREs: one containing VAMP713 and the other with VAMP727 (Ebine *et al*., 2011; Fujiwara *et al*., 2014). To investigate this possibility, I compared the subcellular localization of these R-SNARE proteins with subunits of CORVET and HOPS. VPS39-mRFP exhibited strong colocalization with mGFP-VAMP713 at the contact sites of two vacuoles, whereas mGFP-VPS3 did not (Figure 19). Conversely, mGFP-VPS3 colocalized with TagRFP-VAMP727, but VPS39-mRFP did not (Figure 20). The core complex subunit, mGFP-VPS18, partially colocalized with both R-SNARE molecules (Figure 19, 20). I then investigated whether CORVET and HOPS physically interact with these R-SNAREs. The 9-day-old seedlings expressing mGFP-VAMP727 or mGFP-VAMP713 were subjected to immunoprecipitation followed by mass spectrometry. I detected CORVET-specific subunits but not HOPS-specific subunits in the VAMP727-precipitate, and the VAMP713-precipitate contained only HOPS-specific subunits (Figure 21). Any subunits of these complexes were not co-immunoprecipitated with free GFP. These results indicate that the two endosomal/vacuolar tethering complexes, CORVET and HOPS, mediate distinct membrane fusion events at the vacuole; HOPS acts with the VAMP713-containing SNARE complex to mediate membrane fusion between vacuoles, whereas CORVET promotes membrane fusion between multivesicular endosomes and the vacuole, a process mediated by the SNARE complex involving VAMP727 as its R-SNARE (Ebine *et al*., 2008) (Figure 22).

Chapter 3: Discussion

In this study, I demonstrated that almost all subunits of CORVET and HOPS complexes are co-immunoprecipitated with VPS18, suggesting that CORVET and HOPS complexes are conserved in Arabidopsis. However, my results also demonstrated that these complexes act differently from their animal and yeast counterparts in the uniquely developed plant vacuolar transport system. In budding yeast, CORVET and HOPS regulate a sequential trafficking event during endosomal maturation, which involves Rab conversion mediated by the Mon1-Ccz1 complex, an effector of Vps21 which also acts as an activating factor for Ypt7 (Nordmann *et al*., 2010). This scheme is essentially conserved in metazoa (Balderhaar and Ungermann, 2013), suggesting a conserved regulatory mechanism of vacuolar/lysosomal transport in Opisthokonta. In plants, the vacuolar transport system has uniquely diversified during evolution to produce complex, highly specialized endosomal/vacuolar transport pathways. There are at least three distinct transport pathways operate in vacuolar transport in Arabidopsis, one of which involves both RAB5 and RAB7 whereas another requires only RAB5 (Ebine *et al*., 2014). The latter pathway is responsible for SYP22 transport, which corresponds to the CORVET-dependent transport pathway I identified in this study, as SYP22 also requires CORVET function for vacuolar localization. Together with the plausible involvement of the plant-specific R-SNARE VAMP727 in this pathway, which was suggested by colocalization and interaction of CORVET and VAMP727, I propose a model of the components acting in this pathway in Figure 22. This functional module contains conventional RAB5, CORVET, and the VAMP727-containing SNARE complex, and is likely responsible for fusion between multivesicular endosomes and the vacuolar membrane, based on the observation that VAMP727 mediates the fusion between these

membranes (Ebine *et al*., 2008).

The other module contains RAB7, HOPS, and the VAMP71-containing SNARE complex (Figure 22). This module likely mediates homotypic fusion between vacuoles, considering the colocalization of HOPS components and VAMP71 at the contact sites between vacuoles and the fragmented vacuole phenotype induced by depletion of VAMP71 (Leshem *et al*., 2010). This transport pathway seems to correspond to the RAB5- and RAB7-dependent pathway described in previous work (Ebine *et al*., 2014), given that RAB7 is activated by the SAND/MON1-CCZ1 complex, which also acts as an effector of canonical RAB5 (Cui *et al*., 2014; Ebine *et al*., 2014; Singh *et al*., 2014). Consistently, impairment in RAB5 activation by the *vps9a-2* mutation resulted in altered vacuolar membrane localization of HOPS components; VPS18 and VPS39 exhibited a more uniform distribution than in wild-type plants on the vacuolar membrane (Figure 12). Localized RAB5 activation near the vacuolar membrane could be required for confinement of HOPS distribution, a process that may be mediated by the activating complex SAND/MON1-CCZ1 followed by confined activation of RAB7. Otherwise, unknown components required for localization of HOPS to vacuolar membrane subdomains could be delivered to the vacuole through RAB5-dependent trafficking pathways.

Mutations in genes analyzed in this study, *vps18*, *vps3*, and *vps39* resulted in embryonic lethality with partial defects in gametophytic functions, and similar effects have also been reported for *vps11* and *vcl1/vps16* (Hicks *et al*., 2004; Rojo *et al*., 2001; Tan *et al*., 2017). Intriguingly, *vps41* mutations conferred more severe impacts on male gametophyte functions, resulting in male gametophytic lethality (Hao *et al*., 2016). It is

expected that mutations in core complex components would confer stronger effects, as those mutants would be defective in both CORVET- and HOPS-dependent trafficking pathways. I also confirmed that VPS18, a subunit of the core complex, colocalized with both RAB5 and RAB7, as well as with CORVET- and HOPS-specific subunits. Although the reason of this phenotypic variation is not clear at present, there may be additional gametophyte functions for some of subunits of CORVET and HOPS such as VPS41.

Above, I have shown that both CORVET and HOPS mediate membrane fusion at the vacuole, distinct from their sequential actions during vacuolar/lysosomal transport in animal and yeast cells. This dual-module system for vacuolar membrane fusion may have provided additional options to the plant vacuolar transport system, which has led to the evolution of a novel plant vacuolar transport pathway. This could also have been accomplished by incorporating plant-specific transport machinery components such as VAMP727.

The unique plant-specific organization of the vacuolar transport system may also be associated with plant-specific reorganization of the endocytic pathway. Homotypic early endosomal fusion, which is mediated by RAB5 and CORVET in non-plant systems, is not employed in plants. Instead, the TGN acts as the early endosome in plants (Viotti *et al.*, 2010). Recruitment of the RAB5-CORVET complex to membrane fusion events, distinct from those in non-plant systems, might have led to the plant-specific organization of the endocytic pathway. Further studies on the vacuolar and endocytic transport pathways in basal lineages of plants such as algae, chara, mosses, and liverworts would be effective for reconstituting the evolutionary path that plants followed to develop their unique vacuolar/endosomal system.

Materials and Methods

Plant Materials and Plasmids

Arabidopsis *vps3* (SALK_0428653) and *vps39* (SALK_092095) mutants were obtained from the ABRC. The mutants were backcrossed at least three times to wild-type Arabidopsis (Col-0). The *vps18* mutant and transgenic plants expressing GFP were kindly provided by Dr. M.T. Morita and Dr. S. Mano, respectively (Mano et al., 1999; Niihama et al., 2009). The transgenic plant expressing PTS1-GFP and ARA6-mRFP, or ARA6-mGFP and ARA6-mRFP was kindly gifted by Dr. E. Ito. The *vps9a-2*, *ccz1a*, and *ccz1b* mutants were obtained from lab stocks (Ebine *et al*., 2014; Goh *et al*., 2007). Construction of transgenic plants expressing mRFP-ARA7, Venus-RABG3f, TagRFP-VAMP727, and mRFP-SYP22 expressed under their native promoters were described previously (Ebine *et al*., 2011; Ebine *et al*., 2008; Inada *et al*., 2016). For construction of mGFP-VAMP713 and mGFP-VAMP727, the mutation for monomerization was introduced by PCR mutagenesis to reported constructs of GFP-VAMP713 and GFP-VAMP727, respectively (Ebine *et al*., 2011; Ebine *et al*., 2008). For construction of transgenic plants expressing fluorescently tagged VPS18, VPS3, VPS39, and VAMP713, cDNA for mGFP, Venus, TagRFP, or mRFP was inserted in front of the start or stop codon of each gene. The genomic fragments contained coding regions and 2.0 kb and 1.0 kb of the 5'- and 3'-flanking sequences, respectively, for *VPS18* (At1g12470), 2.0 kb and 0.9 kb of the 5'- and 3'-flanking sequences, respectively, for *VPS3* (At1g22860), and 2.0 kb and 1.0 kb of the 5'- and 3'-flanking sequences, respectively, for *VPS39* (At4g36630). Chimeric genes were subcloned into pBGW or pHGW vectors (Karimi *et al*., 2002). Transformation of Arabidopsis plants was performed by floral dipping using *Agrobacterium tumefaciens* (strain GV3101::pMP90).

Primers

Primers used for genotyping, cloning, and construction in this study are listed in Table 2.

Microscopy

Fluorescence microscopy of root epidermal cells was performed with an LSM780 (Carl Zeiss). For single-color imaging of VPS18, VPS3, and VPS39, I observed homozygous mutant plants whose lethality was rescued by expression of their respective fluorescently tagged proteins. For colocalization analysis using Venus-RABG3f, mutant plants complemented by fluorescently tagged CORVET and HOPS subunits were transformed with *Venus-RABG3f* subcloned into pBGW, and T1 plants were observed. In other multicolor localization analyses, F1 plants obtained by crossing the appropriate transgenic plants were observed. For labeling vacuolar membranes, Arabidopsis roots were incubated in liquid MS medium plus 4 εM FM4-64 for 3 hr at RT.

For observation of embryos, seeds were cleared according to the method described previously (Aida *et al*., 1997) and observed with a fluorescence microscope (model BX51; Olympus) equipped with a confocal scanner unit (model CSU10; Yokogawa Electric) and a cooled CCD camera (model ORCA-AG; Hamamatsu Photonics).

The colocalization analysis between cytoplasmic puncta was performed as described previously (Ito *et al*., 2012). Pearsonôs colocalization coefficients were calculated using PSC Co-localization plug-in (Krebs *et al*., 2010).

Yeast Two Hybrid Assays

For *VPS11, VPS3,* and *VPS39,* the open reading frame was subcloned into pBD-GAL4-

GWRFC and pAD-GAL4-GWRFC provided from T. Demura (Yamaguchi *et al*., 2008). Plasmids containing each *VPS* were introduced into the AH109 yeast strain (Clontech). pBD-GAL4-Cam plasmids containing ARA7 and ARA6 were described in (Goh *et al*., 2007) and (Sakurai *et al*., 2016). Empty vectors were used for negative controls. Transformation was performed independently at least twice, and at least three colonies per transformation were checked for interaction.

Antibodies

Anti-GFP and anti-RAB7 antibodies were from our lab stock (Takemoto *et al*., under revision). Anti-ARA7 and anti-RHA1 antibodies were described in (Goh *et al*., 2007), and (Haas *et al*., 2007), respectively. For detection of RAB5, I used a mixture of anti-ARA7 and anti-RHA1 antibodies at dilutions of 1:200 (anti-ARA7) and 1:100 (anti-RHA1). Anti-GFP and anti-RAB7 were used at 1:100, and anti-rabbit IgG was used at 1:5000 (GE Healthcare).

Immunoprecipitation and Mass Spectrometry

For immunoprecipitation followed by mass spectrometry, whose results are presented in Figure 3, 6-day-old seedlings of transgenic plants expressing GFP or mGFP-VPS18 were soaked in crosslinking buffer [PBS (pH 7.4) and 1 mM dithiobis (succinimidyl propionate) (DSP) (Thermo Fisher Scientific)] for 1 hr at RT. Tris-HCl (pH 7.5) was then added to 20 mM and incubated for 30 min at RT. Samples were ground in lysis buffer supplied in the micro-MACS GFP-tagged protein isolation kit (Miltenyi Biotec), and debris was then removed by centrifugation at 1000 ×*g* for 10 min at 4 °C. Supernatants were incubated for 60 min at 4 °C for solubilization, centrifuged at 20,000 ×*g* for 10 min

at 4 °C, and used for immunoprecipitation according to the manufacturer's instructions. Immunoprecipitates were separated by SDS-PAGE and stained using Flamingo Fluorescent Gel Stain (BIO-RAD). After lanes were cut from the gel, they were dehydrated with acetonitrile for 5 min and dried in a vacuum desiccator. The gel slices were then deoxidized in 10 mM DTT and 25 mM NH_4HCO_3 at 56 °C for 1 hr, washed with 25 mM NH_4HCO_3 for 10 min, and alkylated with 55 mM iodoacetamide and 25 mM NH_4HCO_3 at RT for 45 min. Then, gel slices were washed with 25 mM NH_4HCO_3, dehydrated with 50 % acetonitrile and 25 mM NH_4HCO_3 for 10 min twice, and dried. After incubating with 10 ε g/mL trypsin in 50 mM NH_4HCO_3 on ice for 30 min, excess solution was removed, and the gel slices were incubated at 37 °C overnight. Digested peptides were extracted with 50 % acetonitrile and 5 % CF_3COOH at RT for 30 min, and then extraction was repeated with new extraction solution. The peptides were dissolved in 30 % acetonitrile and 0.1 % formic acid, and then analyzed with Orbitrap Elite (Thermo Fisher Scientific) using Proteome Discoverer (Thermo Fisher Scientific).

For immunoprecipitation followed by Western blotting and mass spectrometry, whose results are presented in Figure 8 and Figure 21, respectively, 9-day-old transgenic seedlings expressing GFP, mGFP-VPS3, VPS39-mGFP, mGFP-VAMP713, or mGFP-VAMP727 were homogenized in grinding buffer (250 mM Sorbitol, 50 mM HEPES pH 7.5, 2 mM EGTA, 0.5 mM $MgCl_2$, and one tablet of cOmplete EDTA-free (Roche) / 50 mL). Lysates were centrifuged at 1,000 ×*g* for 10 min at 4 °C to remove debris. GTPɔS (Sigma) and $MgCl_2$ were then added to the lysate to 0.1 mM and 1 mM, respectively, and incubated for 5 min at RT, followed by incubation for 1 hr at 4 °C. After incubation for 5 min at RT, DSP was added to 1 mM and incubated for 1 hr. at 4 °C. Tris-HCl (pH 7.5) and Triton X-100 were then added to 20 mM and 1 %, respectively, and incubated for 1 hr at

4 °C. Samples were centrifuged at 20,000 ×*g* for 10 min at 4 °C to remove debris, and supernatants were used for immunoprecipitation using the micro-MACS GFP-tagged protein isolation kit (Miltenyi Biotec) according to the manufacturer's instructions, except for the column wash step; the columns were washed 5 times with wash buffer (grinding buffer + 1 % Triton X-100, 1 mM $MgCl_2$ and 0.1 mM GTPɔS).

Figures and Tables

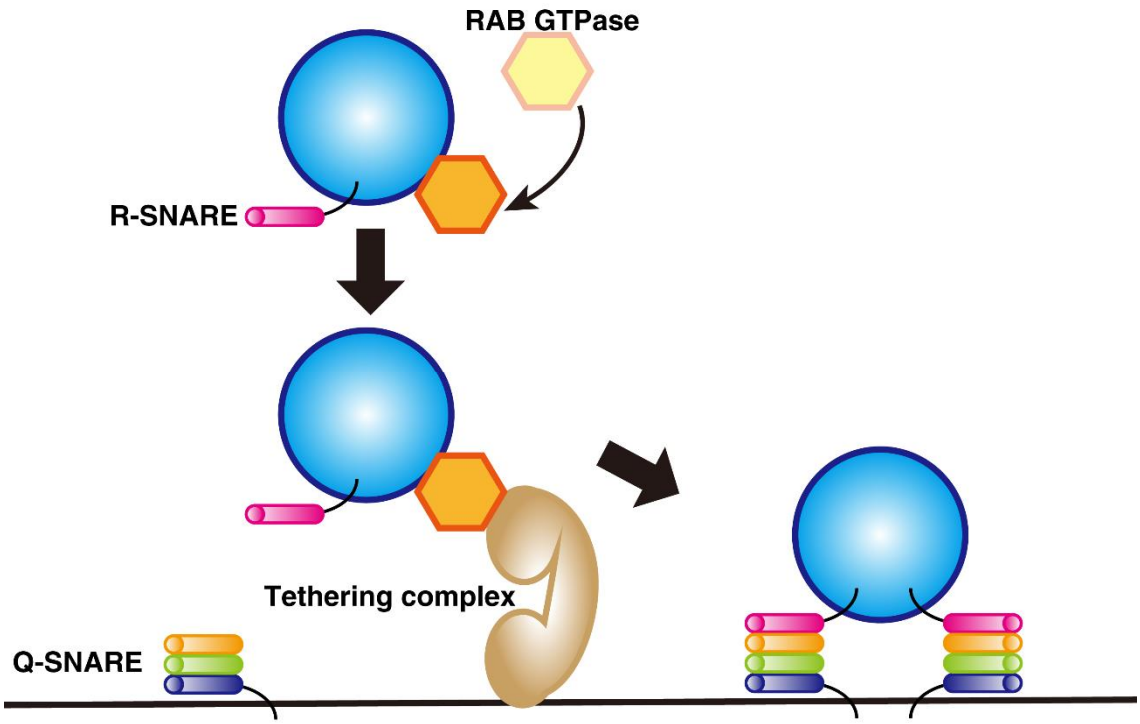

Figure 1. Model of the mechanism of membrane fusion between transport vesicles and target membranes.

Activated RAB GTPases promote tethering transport vesicles to target membranes through recruiting tethering factors, which is followed by SNARE-mediated membrane fusion.

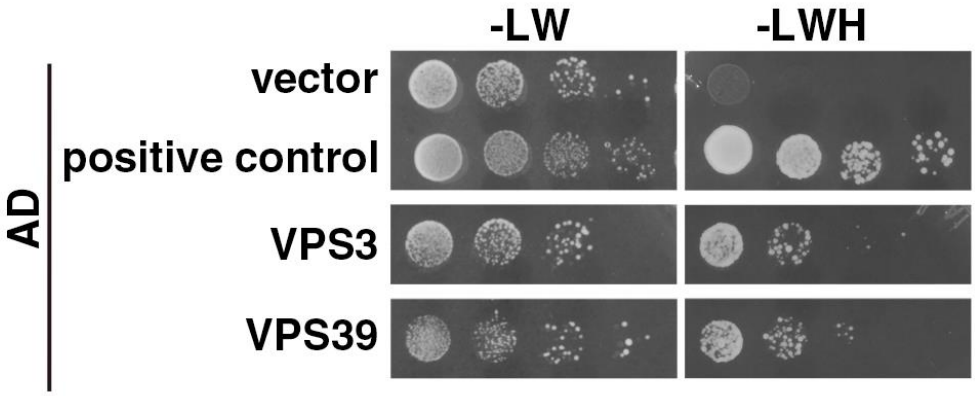

Figure 2. Interactions between VPS11 and VPS3 or VPS39 were tested by yeast two-hybrid assays.

VPS11 was expressed as a fusion protein with the DNA binding domain (BD), and VPS3 and VPS39 were expressed as fusions with a transcriptional activation domain (AD). Interaction between BD-VPS9a and AD-ARA7^{S24N} is shown as positive control. Interactions between two proteins were tested using the *HIS3* reporter gene.

A

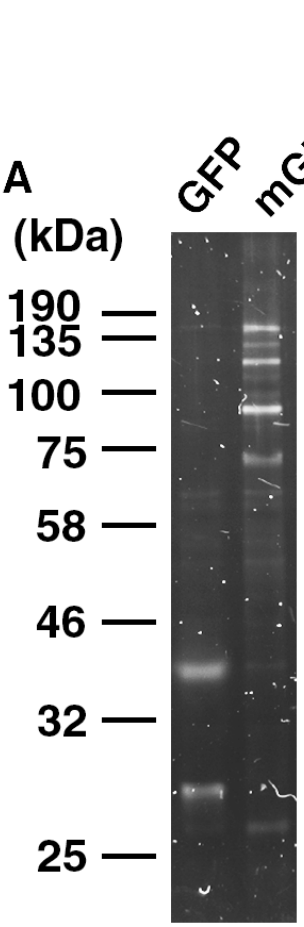

B

AGI code	Score				Assingned name
	1st	2nd	3rd	4th	
AT2G05170	58.6	46.9	62.0	107.9	VPS11
AT2G38020	185.0	123.3	133.2	211.7	VCL1
AT3G54860	138.2	95.6	154.5	187.4	VPS33
AT1G22860	31.6	20.2	49.6	61.5	VPS3
AT4G36630	-	2.3	3.2	1.6	VPS39
AT1G08190	161.9	88.4	126.9	227.0	VPS41

Figure 3. CORVET and HOPS subunits were detected in the immunoprecipitates of mGFP-VPS18.

(A) Flamingo-stained SDS-PAGE gel. Proteins co-precipitated with GFP or mGFP-VPS18 (VPS18) from plant lysates were loaded. (B) Summary of CORVET and HOPS subunits co-precipitated with VPS18 identified by mass spectrometry in four independent experiments. Values in the score column represent XCorr scores, which represent the sum of the ion scores of all peptide sequences matching with the database.

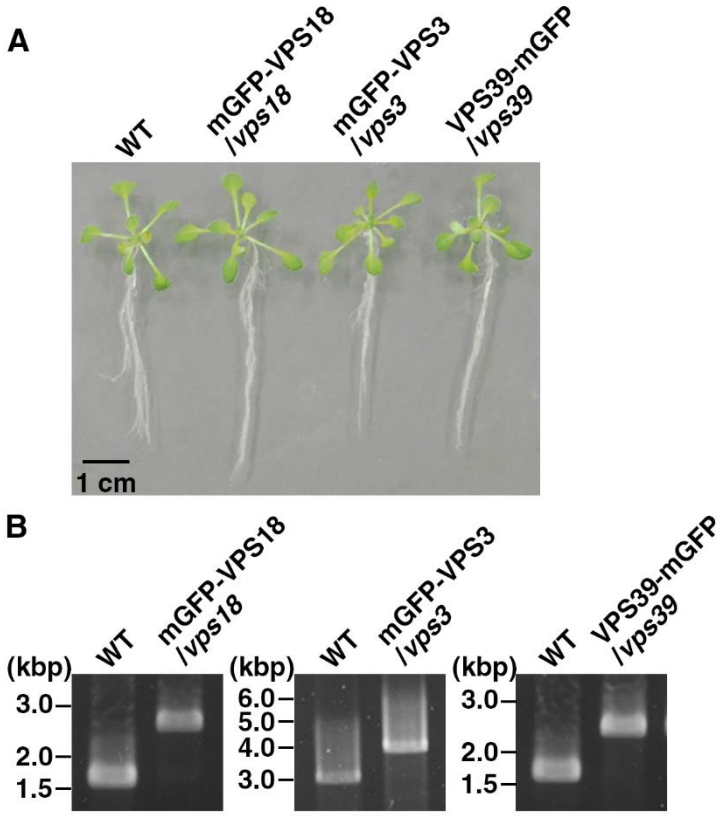

Figure 4. Functionality of fluorescently tagged VPS18, VPS3, and VPS39.

(A) Lethal phenotypes of *vps18*, *vps3*, and *vps39* mutants were rescued by fluorescently tagged VPS18, VPS3, and VPS39, respectively, expressed under control of their endogenous promoters. Representative 14-day-old seedlings are presented. (B) PCR-based genotyping of seedlings presented in (A) indicated that these mutant plants were homozygous for each mutation. Primers are indicated as arrows in Fig. 13.

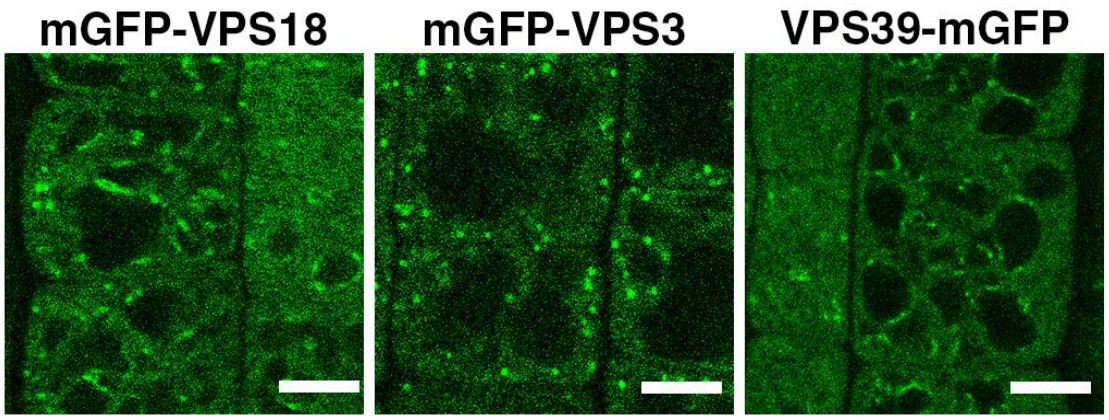

Figure 5. Subcellular localization of mGFP-tagged VPS18, VPS3, and VPS39.

Confocal images of root epidermal cells expressing mGFP-VPS18, VPS3, and VPS39. 5-day-old seedlings were observed. Bars = 5 εm.

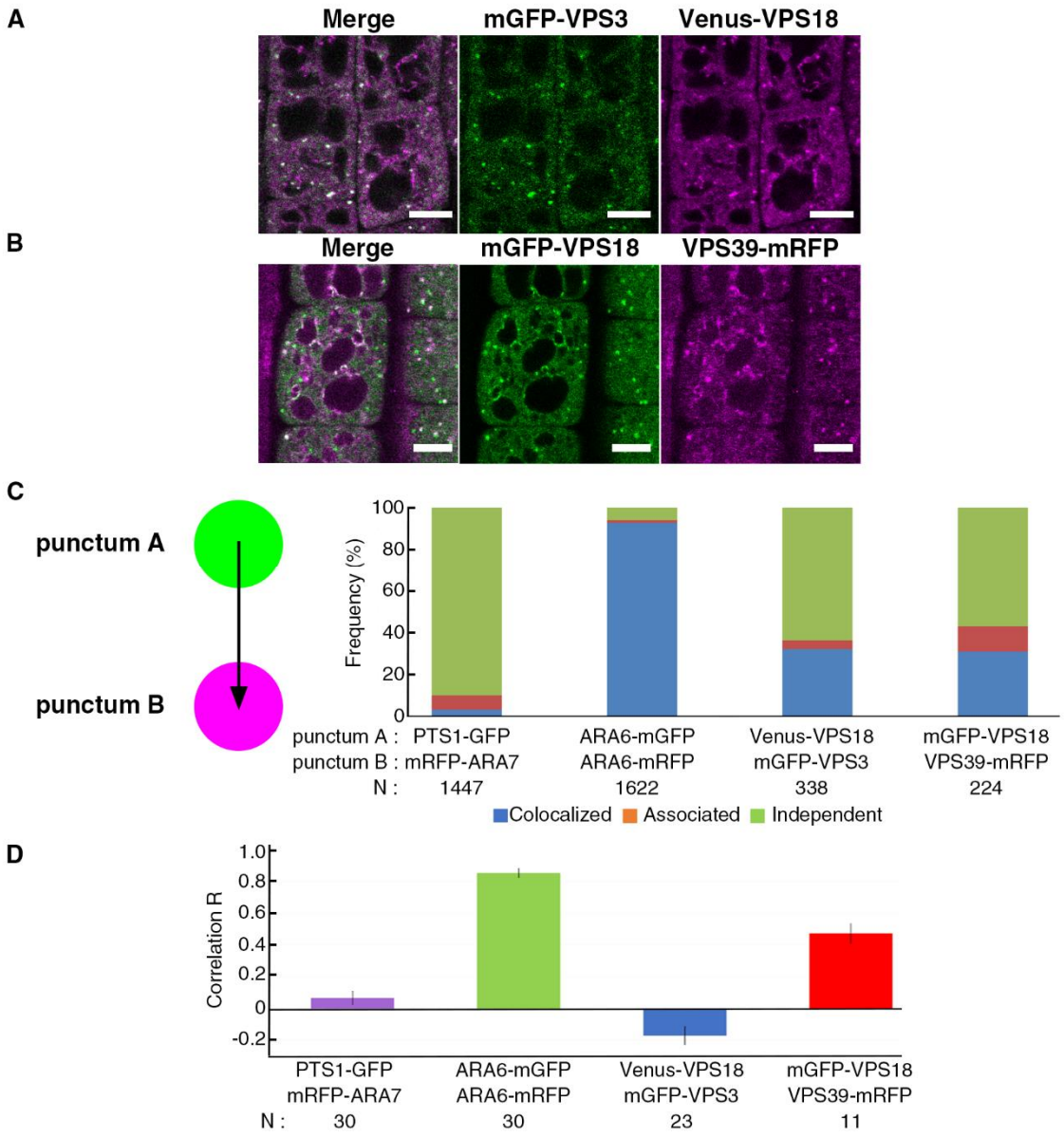

Figure 6. Colocalization analysis of CORVET and HOPS subunits.

(A-B) Confocal images of root epidermal cells expressing Venus-VPS18 and mGFP-VPS3 (A) or mGFP-VPS18 and VPS39-mRFP (B). 5-day-old seedlings were observed. Bars = 5 ε m. (C) Quantitative analysis of the colocalization between proteins tagged with distinct fluorescent proteins localized on punctate compartments (left). The distances from the center of each punctum bearing fluorescently tagged proteins listed at the row

of punctum A to the center of the closest punctum with tagged proteins listed in the row of punctum B were measured and classified as described previously (Ito *et al.*, 2012). In short, distances between two signals were classified into three categories: (i) colocalized; a distance between two centers was below the resolution limit of the objective lens (0.24 μm in this study), (ii) associated; a distance between two centers was less than the sum of the two radii of two signals (< 1 μm in this study), and (iii) independent; a distance between two centers was larger than the sum of the two radii of two signals (> 1 μm in this study). The right stacked bar graphs represent localization relationships between two fluorescently tagged proteins listed in rows punctum A and punctum B. At least 5 individual plants were observed. N, numbers of cytoplasmic dots analyzed. (E) Pearsonôs colocalization coefficients between coexpressed proteins in root epidermal cells. At least 10 individual plants were observed. Error bars indicate SD values. N, numbers of cells analyzed.

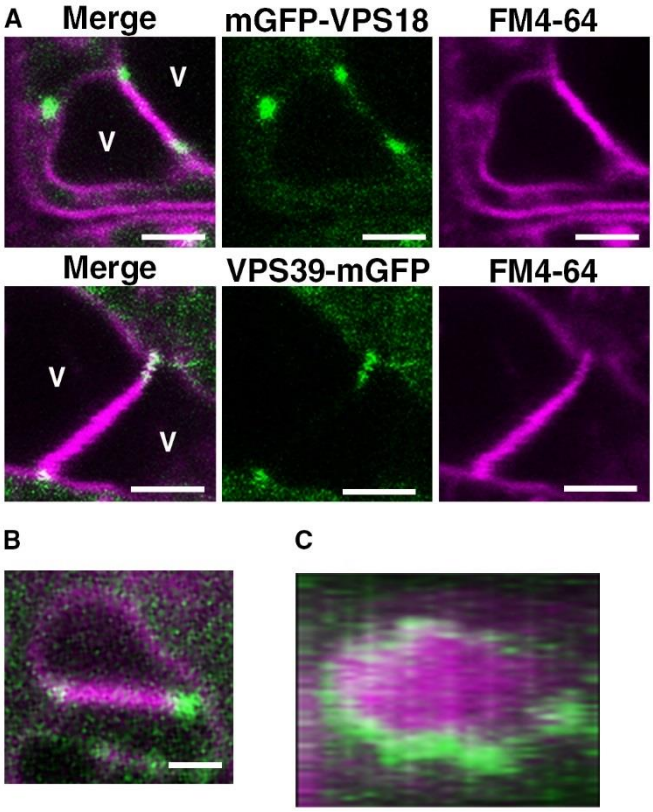

Figure 7. Vertex localization of HOPS subunits.

(A)Transgenic plants expressing mGFP-VPS18 (upper panels) or VPS39-mGFP (lower panels) were stained with FM4-64. GFP fluorescence was frequently observed at the vertex zone of contact sites between two vacuoles. V, vacuole. (B) A 3D projection image of the vertex localization of VPS39-mGFP reconstructed from Z-stack images including the image presented in (A). Root epidermal cells of 5-day-old seedlings were observed. Bars = 2.5 εm.

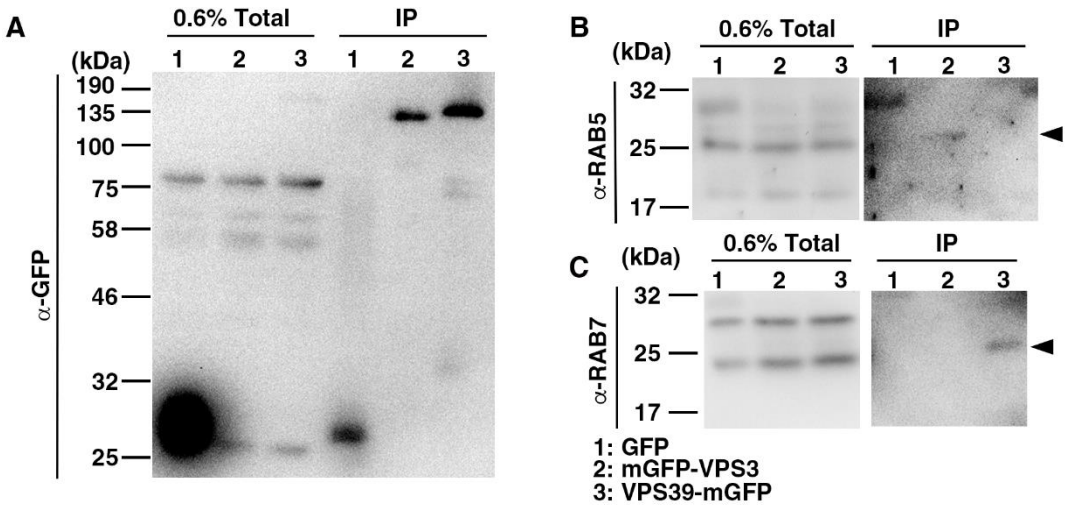

Figure 8. Interaction of CORVET and HOPS with endosomal/vacuolar RAB GTPases.

Co-immunoprecipitation analysis for interaction between tethering complexes and RAB GTPases. Plant lysates prepared from transgenic plants expressing GFP, mGFP-VPS3, or VPS39-mGFP were subjected to immunoprecipitation using the anti-GFP antibody. Precipitates were used for Western blotting using anti-GFP (A), anti-RAB5 (B), and anti-RAB7 (C) antibodies. Arrowheads indicate RAB5 in (B) and RAB7 in (C).

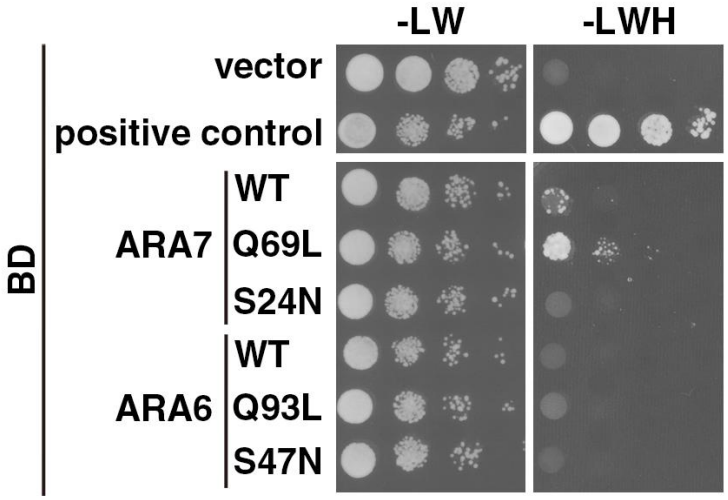

Figure 9. Interactions between VPS3 and RAB5s were tested by yeast two-hybrid assays.

VPS3 was expressed as a fusion protein with the transcriptional activation domain (AD), and ARA7 and ARA6 were expressed as fusions with a DNA binding domain (BD). Interaction between BD-VPS9a and AD-ARA7^{S24N} is shown as a positive control. ARA7^{Q69L} and ARA6^{Q93L} are GTP-fixed forms, and ARA7^{S24N} and ARA6^{S47N} are GDP-fixed forms. Interactions between two proteins were tested using the *HIS3* reporter gene.

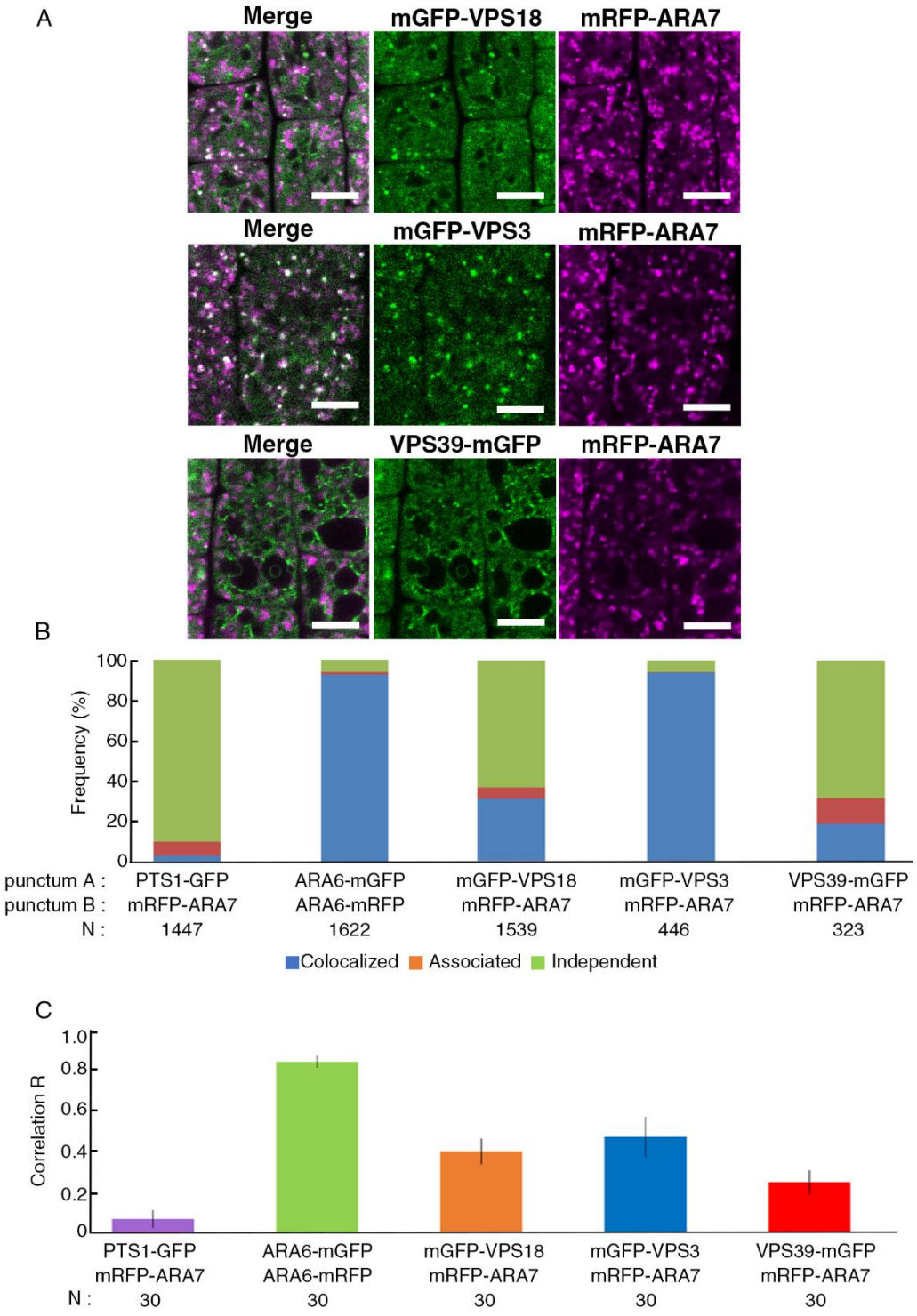

Figure 10. Colocalization between tethering complexes and RAB5.

(A) Root epidermal cells of 5-day-old seedlings co-expressing mRFP-ARA7 and mGFP-VPS18, mGFP-VPS3, or VPS39-mGFP. Bars = 5 ε m. (B) Stacked bar graphs

represent localization relationships between two fluorescently tagged proteins listed in rows punctum A and punctum B. At least 5 individual plants were observed. N, numbers of cytoplasmic dots analyzed. (D) Pearsonôs colocalization coefficients between coexpressed proteins in root epidermal cells. At least 10 individual plants were observed. Error bars indicate SD values. N, numbers of cells analyzed.

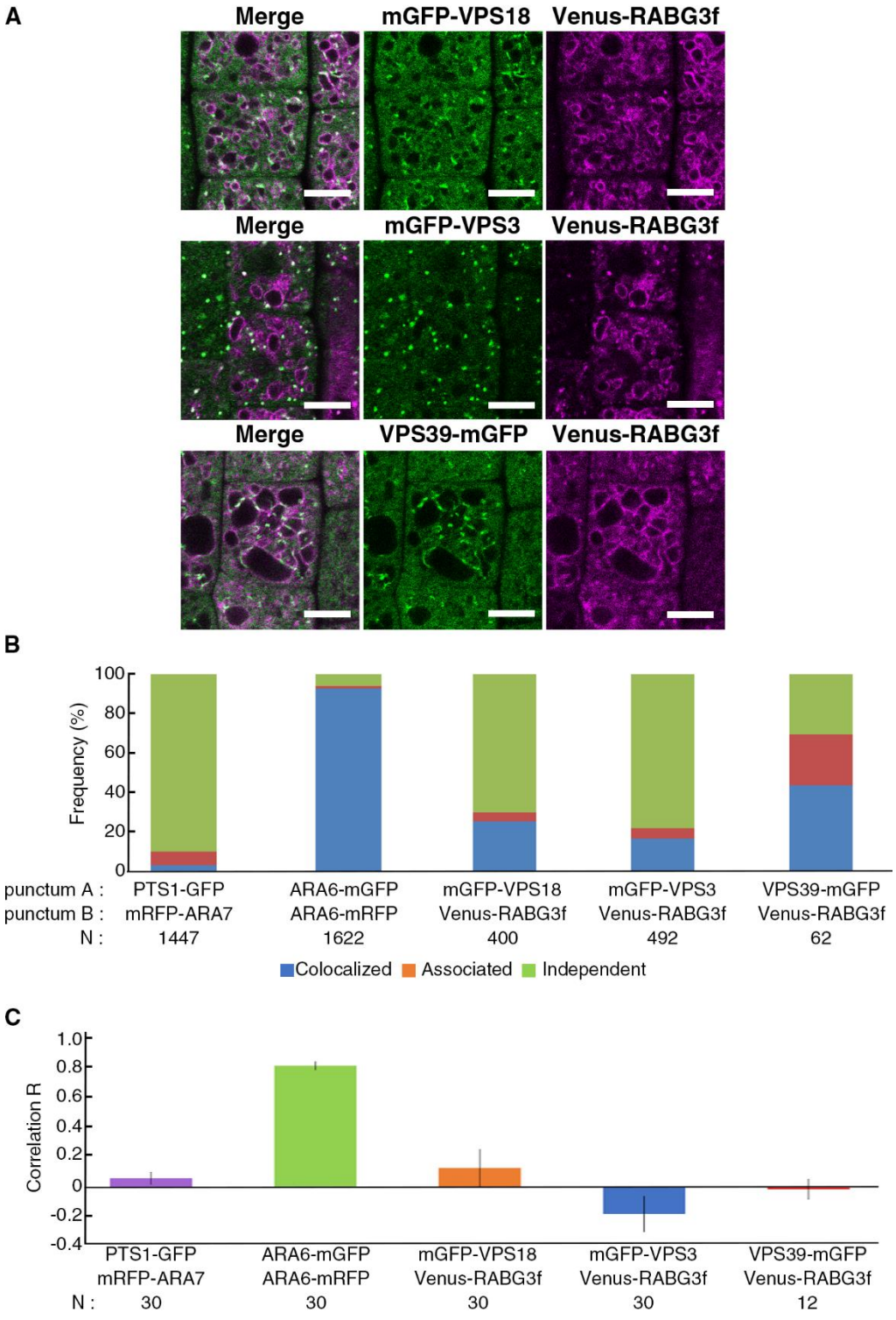

Figure 11. Colocalization between tethering complexes and RAB5.

(A) 5-day-old seedlings co-expressing Venus-RABG3f and mGFP-VPS18, mGFP-VPS3,

or VPS39-mGFP (E) were observed. Bars = 5 εm. (B) Stacked bar graphs represent localization relationships between two fluorescently tagged proteins listed in rows punctum A and punctum B. At least 5 individual plants were observed. N, numbers of cytoplasmic dots analyzed. (C) Pearsonôs colocalization coefficients between coexpressed proteins in root epidermal cells. At least 5 individual plants were observed. Error bars indicate SD values. N, numbers of cells analyzed.

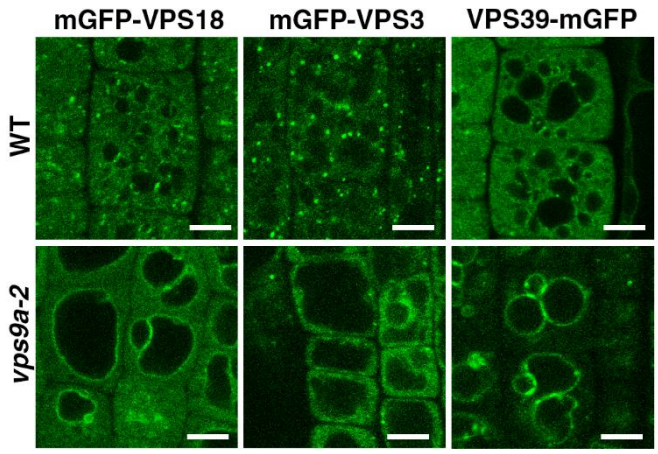

Figure 12. Effects of defective activation of RAB5 on localization of CORVET and HOPS.

mGFP-VPS18, mGFP-VPS3, and VPS39-mGFP were expressed in *vps9a-2* and observed in root epidermal cells of 5-day-old seedlings. Bars = 5 ε m.

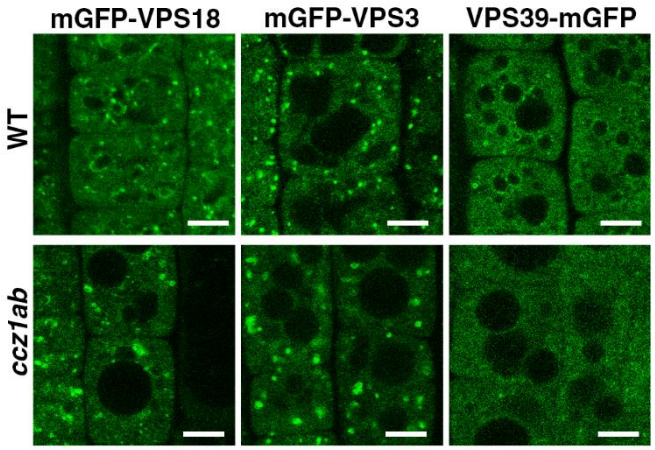

Figure 13. Effects of defective activation of RAB7 on localization of CORVET and HOPS.

mGFP-VPS18, mGFP-VPS3, and VPS39-mGFP were expressed in *ccz1ab* and observed in root epidermal cells of 5-day-old seedlings. Bars = 5 ε m.

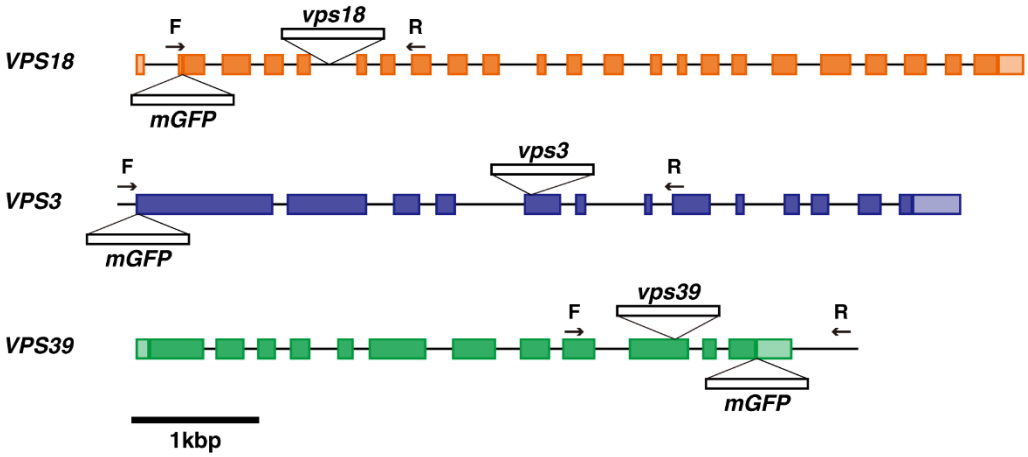

Figure 14. Schematics of *VPS18*, *VPS3,* and *VPS39* gene structures and positions of T-DNA insertions.

Arrows indicate positions of primers used in PCR-based genotyping presented in Fig. 3.

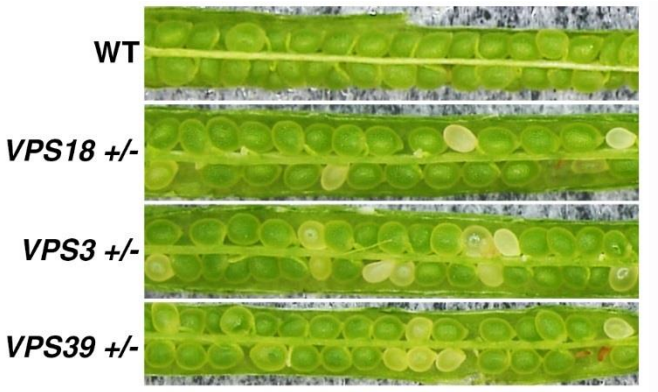

Figure 15. The mutants of CORVET and HOPS subunits exhibited seed defects.

Siliques collected from Arabidopsis plants with the indicated genotypes are shown. The mutant seeds exhibit a yellowish appearance.

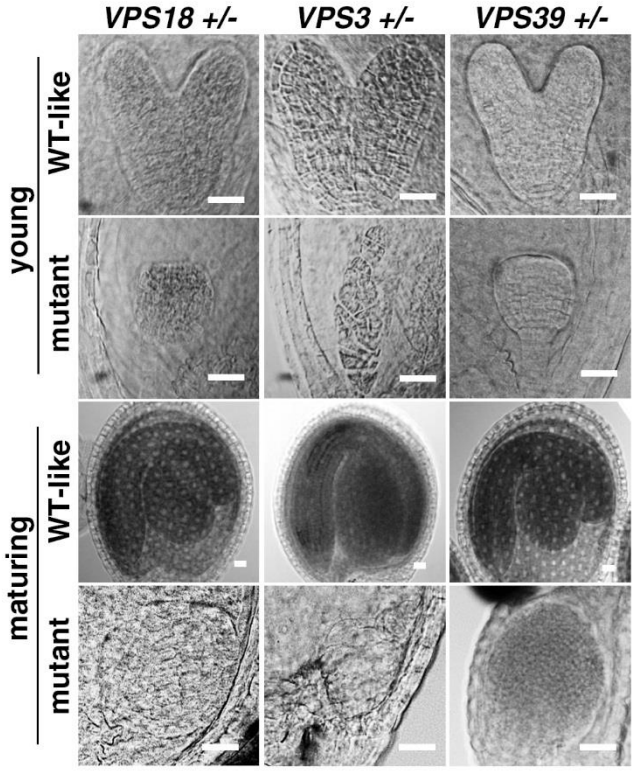

Figure 16. The mutants of CORVET and HOPS subunits exhibited embryonic defects.

Nomarski images of cleared embryos observed in young (upper rows) and maturing (lower rows) siliques collected from plants with the indicated genotypes. Siblings in the same siliques with wild type-like (WT-like) and aberrant appearance (mutant) are presented. Bars = 20 εm.

Parent (male × female)	Progeny		Transmission efficiency
	+/+	+/-	
VPS18+/- × WT	88	31	35.2%
WT × *VPS18*+/-	61	58	95.1%
VPS3+/- × WT	108	33	30.1%
WT × *VPS3*+/-	87	81	93.1%
VPS39+/- × WT	102	37	36.3%
WT × *VPS39*+/-	90	66	73.3%

Tables 1. Transmission of mutations in CORVET and HOPS subunit genes through male and female gametophytes

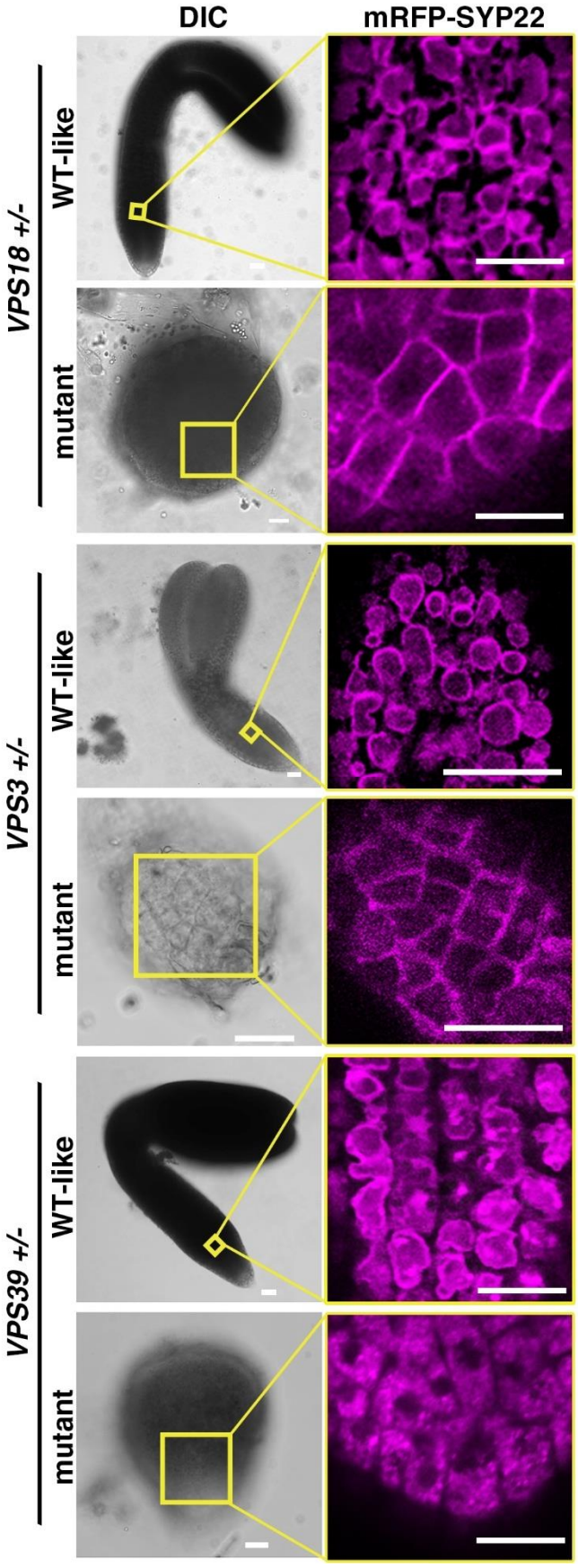
DIC
mRFP-SYP22
VPS18 +/-
WT-like
mutant
VPS3 +/-
WT-like
mutant
VPS39 +/-
WT-like
mutant

Figure 17. Defective CORVET and HOPS complexes confer distinct effects on SYP22 transport.

mRFP-SYP22 was expressed in plants with the indicated genotypes, and its localization was observed in developing embryos. Siblings in the same siliques with wild type-like (WT-like) and aberrant appearance (mutant) were observed. Areas in yellow squares in Nomarski images (left panels) were observed by confocal microscopy (right panels). Bars = 20 εm.

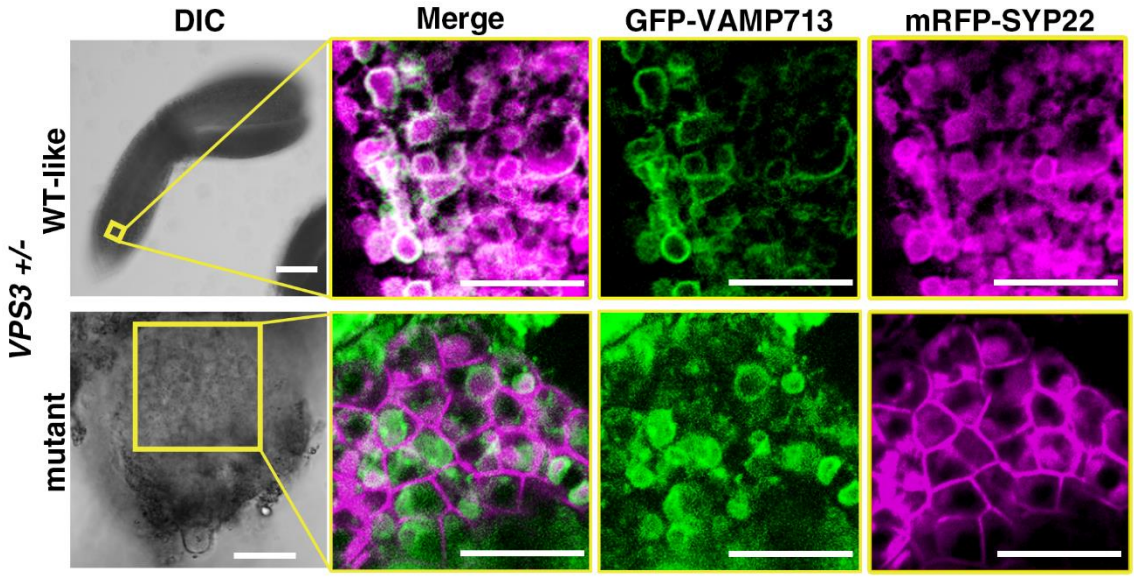

Figure 18. Effects of *vps3* on transport of SYP22 and VAMP713.

GFP-VAMP713 and mRFP-SYP22 were co-expressed in VPS3$^{+/-}$ plants, and their localization was observed in sibling embryos with WT-like and aberrant morphology. Areas of DIC images indicated with yellow squares were observed with a confocal microscope. Bars = 20 ε m.

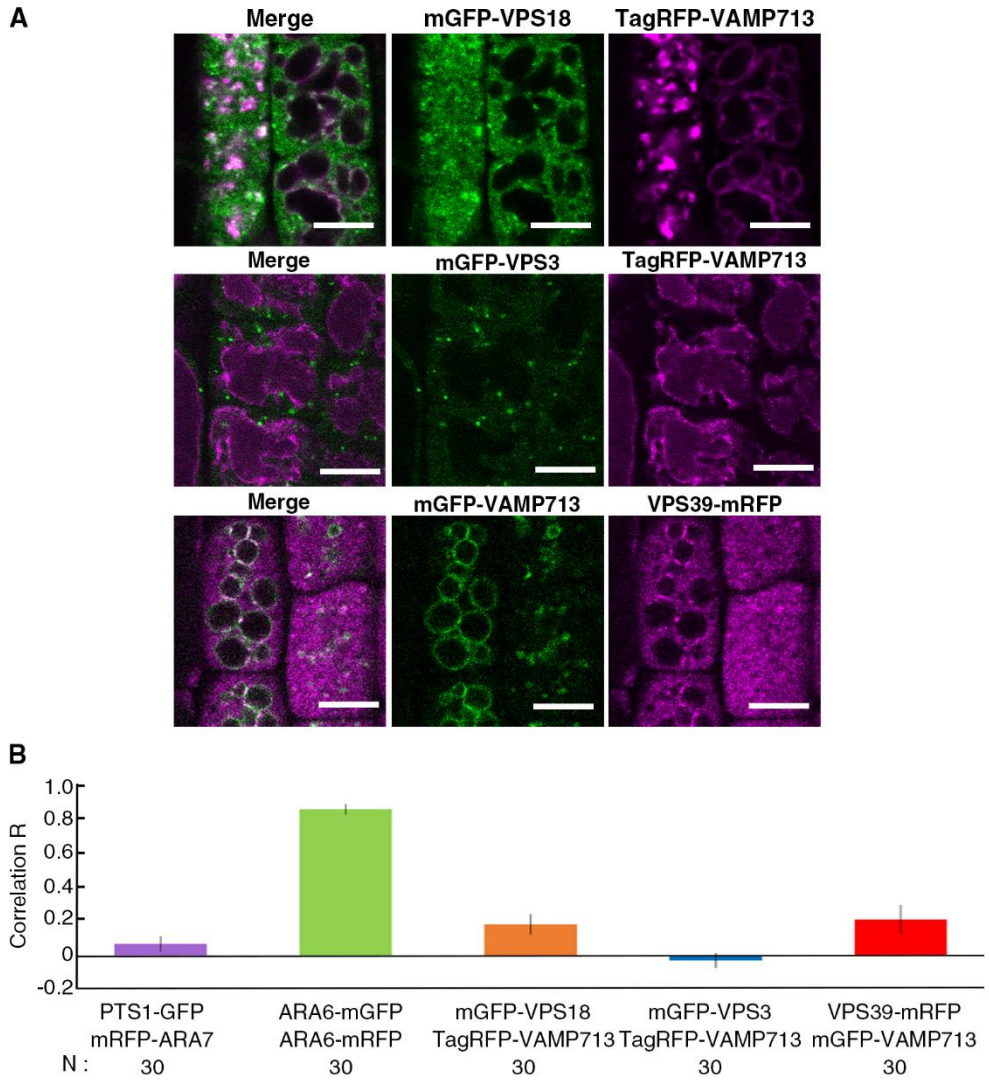

Figure 19. Colocalization between tethering complexes and VAMP713.

(A) Fluorescently-tagged VAMP7113 was co-expressed with mGFP-VPS18, mGFP-VPS3, or VPS39-mRFP. 5-day-old seedlings were observed. Bars = 5 ε m. (B) Pearsonôs colocalization coefficients between coexpressed proteins in root epidermal cells. At least 10 individual plants were observed. Error bars indicate SD values. N, numbers of cells analyzed. Colocalization analysis of cytoplasmic punctate structures was not applicable, because VAMP713 rarely localized to dot-shaped structures.

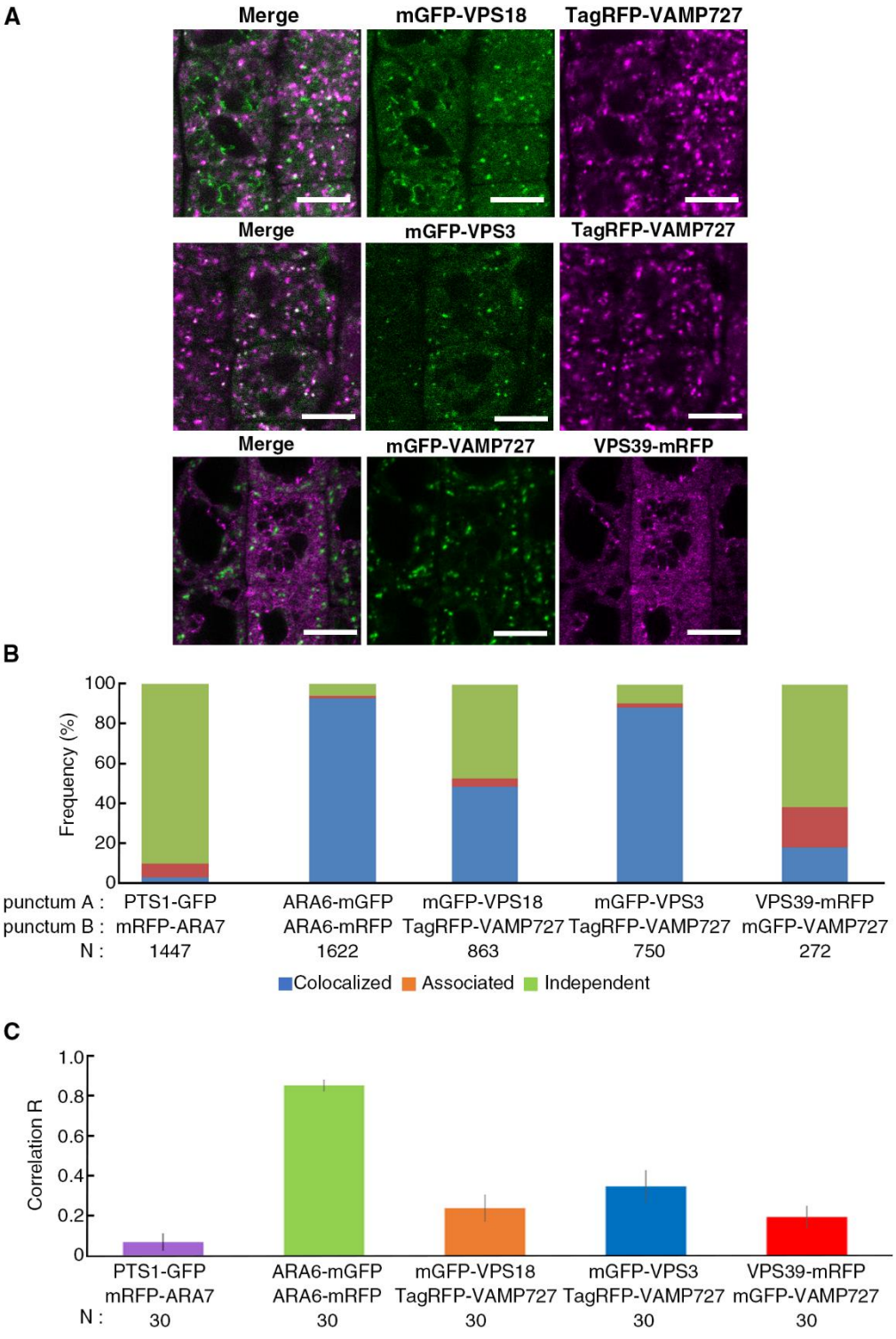

Figure 20. Colocalization between tethering complexes and VAMP727.

(A) Fluorescently-tagged VAMP7113 was co-expressed with mGFP-VPS18, mGFP-

VPS3 or VPS39-mRFP. 5-day-old seedlings were observed. Bars = 5 ε m. (B) Stacked bar graphs represent localization relationships between two fluorescently tagged proteins listed in rows punctum A and punctum B. At least 5 individual plants were observed. N, numbers of cytoplasmic dots analyzed. (C) Pearsonôs colocalization coefficients between coexpessed proteins in root epidermal cells. At least 10 individual plants were observed. Error bars indicate SD values. N, numbers of cells analyzed.

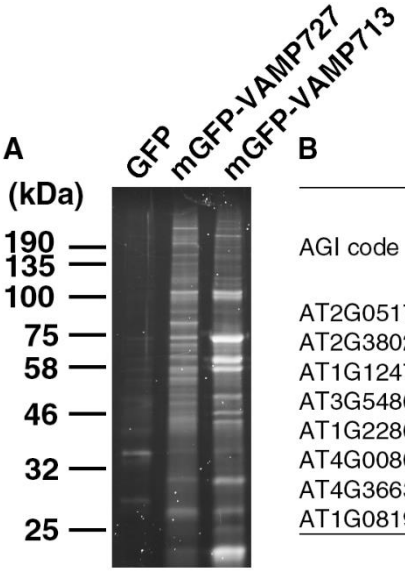

B

AGI code	Score mGFP-VAMP727 1st	Score mGFP-VAMP727 2nd	Score mGFP-VAMP713 1st	Score mGFP-VAMP713 2nd	Assingned name	
AT2G05170	12.5	4.4	48.2	46.2	VPS11	Class C Core
AT2G38020	11.7	-	46.2	45.3	VCL1	
AT1G12470	28.6	16.3	70.9	65.6	VPS18	
AT3G54860	9.4	5.7	27.8	35.4	VPS33	
AT1G22860	11.9	6.4	-	-	VPS3	CORVET specific
AT4G00800	10.7	18.3	-	-	VPS8	
AT4G36630	-	-	49.3	37.2	VPS39	HOPS specific
AT1G08190	-	-	31.6	41.9	VPS41	

Figure 21. CORVET and HOPS were co-immunoprecipitated with distinct SNAREs.

(A) Flamingo-stained SDS-PAGE gel. Proteins co-precipitated with GFP, mGFP-VAMP727, or mGFP-VAMP713 from plant lysates were loaded. (B) Summary of CORVET and HOPS subunits co-precipitated with VAMP proteins identified by mass spectrometry in two independent experiments. Values in the score column represent XCorr scores, which represent the sum of the ion scores of all peptide sequences matching with the database.

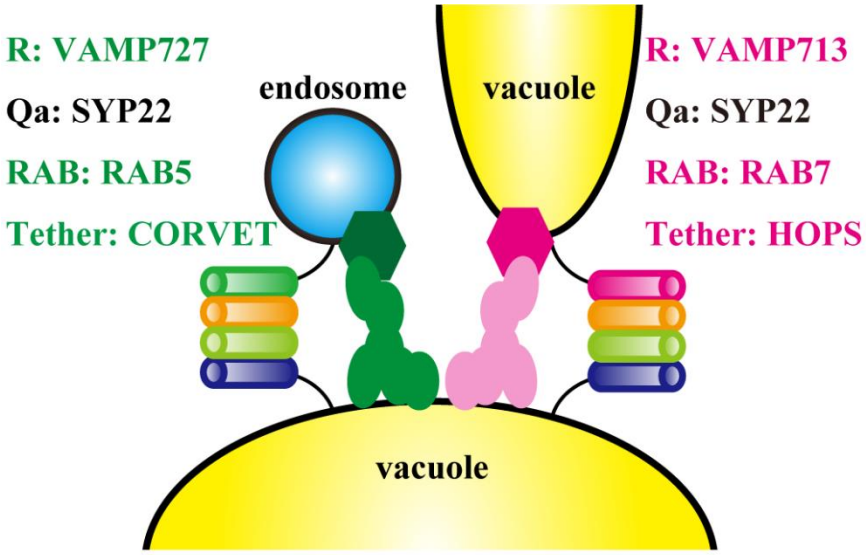

Figure 22. Schematic illustration of tethering-fusion modules acting in vacuolar transport in Arabidopsis cells.

Two endosomal/vacuolar tethering complexes, CORVET and HOPS, mediate distinct membrane fusion events at the vacuole; CORVET mediates membrane fusion between multivesicular endosomes and the vacuole, in coordination with RAB5 and the VAMP727-containing SNARE complex, whereas HOPS acts with the VAMP713-containing SNARE complex and RAB7 to mediate membrane fusion between vacuoles.

Table 2. The primer list used in this paper

Name	Sequence	Use
VPS18-genomic-F	5ô-CACCTGGTTGCAGAGATGTTTCAG-3ô	Cloning
VPS18-genomic-R	5ô-CTAGCGAAAAGTCCTGCAAC-3ô	Cloning
VPS3-genomic-F	5ô-CACCTCAGACTATAGCTTATCAAGTTGAA-3ô	Cloning
VPS3-genomic-R	5ô-CATAAACCAAAACAGCTTCA-3ô	Cloning
VPS39-genomic-F	5ô-CACCGAAGGAATGCTCACCAACTC-3ô	Cloning
VPS39-genomic-R	5ô-TACATTGTGTTCTTTCTTTAGCTTG-3ô	Cloning
VPS18-CDS-F	5ô-CACCATGGATCAAGGAAGGCAAGTG-3ô	Cloning
VPS18-CDS-R	5ô-TCAAACAGGCAAAGAAATGGTC-3ô	Cloning
VPS3-CDS-F	5ô-CACCATGTCCAAATCTCGGGCAGTTG-3ô	Cloning
VPS3-CDS-R	5ô-CTACCGGTTAACTAACCAACCG-3ô	Cloning
VPS39-CDS-F	5ô-CACCATGGTTCACAACGCTTATGATT-3ô	Cloning
VPS39-CDS-R	5ô-TCATCGTCTTCTTCCATGTGT-3ô	Cloning
XFP-VPS18-F	5ô-AAGGGAGGAAGTGGAATGGATCAAGGAAGGCAAG-3ô	Construction
XFP-VPS18-R	5ô-GCCCTTGCTCACCATCTTCTTCCTCTCTTAATCAAAAACT-3ô	Construction
mGFP-VPS3-F	5ô-GACGAGCTGTACAAGATGTCCAAATCTCGGGCAG-3ô	Construction
mGFP-VPS3-R	5ô-GCCCTTGCTCACCATGACCTAAACCAGATATACGA-3ô	Construction
VPS39-mGFP-F	5ô-GACGAGCTGTACAAGTGAGGTAATCATCAATTACTGTAACA-3ô	Construction
VPS39-mGFP-R	5ô-CATTCCACTTCCTCCTCGTCTTCTTCCATGTGTTG-3ô	Construction
VPS39-mRFP-F	5ô-CACTCCACCGGCGCCTGAGGTAATCATCAATTACTGTAACA-3ô	Construction
VPS39-mRFP-R	5ô-CATTCCACTTCCTCCTCGTCTTCTTCCATGTGTTG-3ô	Construction
TagR-VAMP713-F	5ô-GGAGGAGGTAGTGGCGGCGCGATCATATTTGCGTTGGT-3ô	Construction
TagR-VAMP713-R	5ô-GCCCTTAGACACCATCTACTCCGGCACCTTGTTCC-3ô	Construction
mGFP-Nterm-F	5ô-ATGGTGAGCAAGGGCGAGGA-3ô	Construction
mGFP-Nterm-R	5ô-TCCACTTCCTCCCTTGTACAGCTCGTCCATGC-3ô	Construction
mGFP-Cterm-F	5ô-GGAGGAAGTGGAATGGTGAGCAAGGGCGAGGA-3ô	Construction
mGFP-Cterm-R	5ô-CTTGTACAGCTCGTCCATGC-3ô	Construction
mRFP-F	5ô-GGAGGAAGTGGAATGGCCTCCTCCGAGGACG-3ô	Construction
mRFP-R	5ô-GGCGCCGGTGGAGTGGC-3ô	Construction
TagRFP-F	5ô-ATGGTGTCTAAGGGCGAAGA-3ô	Construction
TagRFP-R	5ô-GCCGCCACTACCTCCTCCATTAAGTTTGTGCCCCAGTT-3ô	Construction
vps18-F	5ô-AACTTCCTGAAGCCTTCAAGG-3ô	Genotyping
vps18-R	5ô-CAGGCTTGACTGCTTCAGTTC-3ô	Genotyping
vps18-complement-F	5ô-AGTTTTTGATTAAGAGAGGAAGAAG-3ô	Genotyping

vps18-complement-R	5ô-CAGGCTTGACTGCTTCAGTTC-3ô	Genotyping
vps3-F	5ô-CCAGTGAGGGAGGGAATAGAC-3ô	Genotyping
vps3-R	5ô-ACCATTGGAAGTACCTGGCC-3ô	Genotyping
vps3-complement-F	5ô-TGTACATCGTATATCTGGTTTAGGTC-3ô	Genotyping
vps3-complement-R	5ô-ACCATTGGAAGTACCTGGCC-3ô	Genotyping
vps39-F	5ô-CTTTGTTGAAGCGTCTTCCAC-3ô	Genotyping
vps39-R	5ô-ATCTTGTTGGAGGATGTCGT-3ô	Genotyping
vps39-complement-F	5ô-CTTTGTTGAAGCGTCTTCCAC-3ô	Genotyping
vps39-complement-R	5ô-ATCTTGTTGGAGGATGTCGT-3ô	Genotyping
vps9a-2-F	5ô-GCTCCTCGTGATAAGCTTGTG-3ô	Genotyping
vps9a-2-R	5ô-TTGGAATCACGTTCTTCATCC-3ô	Genotyping
ccz1a-F	5ô-ATACATTGGCAGGTTGTGGAG-3ô	Genotyping
ccz1a-R	5ô-AATGGCATTTGTAGGCATCAG-3ô	Genotyping
ccz1b-F	5ô-TTCAGGTGGTACATTGCCTTC-3ô	Genotyping
ccz1b-R	5ô-AAACCGTCAAGGGTCAAGTTC-3ô	Genotyping
LB_SALK	5ô-ATTTTGCCGATTTCGGAAC-3ô	Genotyping
LB_SAIL	5ô-TCGGAACCACCATCAAACAG-3ô	Genotyping
LB_GABI	5ô-ATATTGACCATCATACTCATTGC-3ô	Genotyping

References

Aida, M., T. Ishida, H. Fukaki, H. Fujisawa, and M. Tasaka. 1997. Genes involved in organ separation in Arabidopsis: an analysis of the cup-shaped cotyledon mutant. *The Plant cell*. 9:841-857.

Anuntalabhochai, S., N. Terryn, M. Van Montagu, and D. Inze. 1991. Molecular characterization of an *Arabidopsis thaliana* cDNA encoding a small GTP-binding protein, Rha1. *The Plant journal : for cell and molecular biology*. 1:167-174.

Balderhaar, H.J., and C. Ungermann. 2013. CORVET and HOPS tethering complexes - coordinators of endosome and lysosome fusion. *Journal of cell science*. 126:1307-1316.

Cabrera, M., H. Arlt, N. Epp, J. Lachmann, J. Griffith, A. Perz, F. Reggiori, and C. Ungermann. 2013. Functional separation of endosomal fusion factors and the class C core vacuole/endosome tethering (CORVET) complex in endosome biogenesis. *The Journal of biological chemistry*. 288:5166-5175.

Cabrera, M., L. Langemeyer, M. Mari, R. Rethmeier, I. Orban, A. Perz, C. Brocker, J. Griffith, D. Klose, H.J. Steinhoff, F. Reggiori, S. Engelbrecht-Vandre, and C. Ungermann. 2010. Phosphorylation of a membrane curvature-sensing motif switches function of the HOPS subunit Vps41 in membrane tethering. *The Journal of cell biology*. 191:845-859.

Caplan, S., L.M. Hartnell, R.C. Aguilar, N. Naslavsky, and J.S. Bonifacino. 2001. Human Vam6p promotes lysosome clustering and fusion in vivo. *The Journal of cell biology*. 154:109-122.

Cui, Y., Q. Zhao, C. Gao, Y. Ding, Y. Zeng, T. Ueda, A. Nakano, and L. Jiang. 2014. Activation of the Rab7 GTPase by the MON1-CCZ1 Complex Is Essential for

PVC-to-Vacuole Trafficking and Plant Growth in Arabidopsis. *The Plant cell*. 26:2080-2097.

Ebine, K., M. Fujimoto, Y. Okatani, T. Nishiyama, T. Goh, E. Ito, T. Dainobu, A. Nishitani, T. Uemura, M.H. Sato, H. Thordal-Christensen, N. Tsutsumi, A. Nakano, and T. Ueda. 2011. A membrane trafficking pathway regulated by the plant-specific RAB GTPase ARA6. *Nature cell biology*. 13:853-859.

Ebine, K., T. Inoue, J. Ito, E. Ito, T. Uemura, T. Goh, H. Abe, K. Sato, A. Nakano, and T. Ueda. 2014. Plant vacuolar trafficking occurs through distinctly regulated pathways. *Current biology : CB*. 24:1375-1382.

Ebine, K., Y. Okatani, T. Uemura, T. Goh, K. Shoda, M. Niihama, M.T. Morita, C. Spitzer, M.S. Otegui, A. Nakano, and T. Ueda. 2008. A SNARE complex unique to seed plants is required for protein storage vacuole biogenesis and seed development of *Arabidopsis thaliana*. *The Plant cell*. 20:3006-3021.

Fujiwara, M., T. Uemura, K. Ebine, Y. Nishimori, T. Ueda, A. Nakano, M.H. Sato, and Y. Fukao. 2014. Interactomics of Qa-SNARE in *Arabidopsis thaliana*. *Plant & cell physiology*. 55:781-789.

Goh, T., W. Uchida, S. Arakawa, E. Ito, T. Dainobu, K. Ebine, M. Takeuchi, K. Sato, T. Ueda, and A. Nakano. 2007. VPS9a, the common activator for two distinct types of Rab5 GTPases, is essential for the development of *Arabidopsis thaliana*. *The Plant cell*. 19:3504-3515.

Haas, T.J., M.K. Sliwinski, D.E. Martinez, M. Preuss, K. Ebine, T. Ueda, E. Nielsen, G. Odorizzi, and M.S. Otegui. 2007. The Arabidopsis AAA ATPase SKD1 is involved in multivesicular endosome function and interacts with its positive regulator LYST-INTERACTING PROTEIN5. *The Plant cell*. 19:1295-1312.

Hao, L., J. Liu, S. Zhong, H. Gu, and L.J. Qu. 2016. AtVPS41-mediated endocytic pathway is essential for pollen tube-stigma interaction in Arabidopsis. *Proceedings of the National Academy of Sciences of the United States of America*. 113:6307-6312.

Hicks, G.R., E. Rojo, S. Hong, D.G. Carter, and N.V. Raikhel. 2004. Geminating pollen has tubular vacuoles, displays highly dynamic vacuole biogenesis, and requires VACUOLESS1 for proper function. *Plant physiology*. 134:1227-1239.

Huizing, M., A. Didier, J. Walenta, Y. Anikster, W.A. Gahl, and H. Kramer. 2001. Molecular cloning and characterization of human VPS18, VPS 11, VPS16, and VPS33. *Gene*. 264:241-247.

Inada, N., S. Betsuyaku, T.L. Shimada, K. Ebine, E. Ito, N. Kutsuna, S. Hasezawa, Y. Takano, H. Fukuda, A. Nakano, and T. Ueda. 2016. Modulation of Plant RAB GTPase-Mediated Membrane Trafficking Pathway at the Interface Between Plants and Obligate Biotrophic Pathogens. *Plant & cell physiology*. 57:1854-1864.

Ito, E., M. Fujimoto, K. Ebine, T. Uemura, T. Ueda, and A. Nakano. 2012. Dynamic behavior of clathrin in *Arabidopsis thaliana* unveiled by live imaging. *The Plant journal : for cell and molecular biology*. 69:204-216.

Karimi, M., D. Inze, and A. Depicker. 2002. GATEWAY vectors for Agrobacterium-mediated plant transformation. *Trends in plant science*. 7:193-195.

Klinger, C.M., M.J. Klute, and J.B. Dacks. 2013. Comparative Genomic Analysis of Multi-Subunit Tethering Complexes Demonstrates an Ancient Pan-Eukaryotic Complement and Sculpting in Apicomplexa. *PloS one*. 8.

Krebs, M., D. Beyhl, E. Gorlich, K.A. Al-Rasheid, I. Marten, Y.D. Stierhof, R. Hedrich, and K. Schumacher. 2010. Arabidopsis V-ATPase activity at the

tonoplast is required for efficient nutrient storage but not for sodium accumulation. *Proceedings of the National Academy of Sciences of the United States of America*. 107:3251-3256.

Lachmann, J., E. Glaubke, P.S. Moore, and C. Ungermann. 2014. The Vps39-like TRAP1 is an effector of Rab5 and likely the missing Vps3 subunit of human CORVET. *Cellular logistics*. 4:e970840.

Leshem, Y., Y. Golani, Y. Kaye, and A. Levine. 2010. Reduced expression of the v-SNAREs AtVAMP71/AtVAMP7C gene family in Arabidopsis reduces drought tolerance by suppression of abscisic acid-dependent stomatal closure. *Journal of experimental botany*. 61:2615-2622.

Mano, S., M. Hayashi, and M. Nishimura. 1999. Light regulates alternative splicing of hydroxypyruvate reductase in pumpkin. *The Plant journal : for cell and molecular biology*. 17:309-320.

Nickerson, D.P., C.L. Brett, and A.J. Merz. 2009. Vps-C complexes: gatekeepers of endolysosomal traffic. *Current opinion in cell biology*. 21:543-551.

Niihama, M., N. Takemoto, Y. Hashiguchi, M. Tasaka, and M.T. Morita. 2009. ZIP genes encode proteins involved in membrane trafficking of the TGN-PVC/vacuoles. *Plant & cell physiology*. 50:2057-2068.

Nordmann, M., M. Cabrera, A. Perz, C. Brocker, C. Ostrowicz, S. Engelbrecht-Vandre, and C. Ungermann. 2010. The Mon1-Ccz1 complex is the GEF of the late endosomal Rab7 homolog Ypt7. *Current biology : CB*. 20:1654-1659.

Ostrowicz, C.W., C. Brocker, F. Ahnert, M. Nordmann, J. Lachmann, K. Peplowska, A. Perz, K. Auffarth, S. Engelbrecht-Vandre, and C. Ungermann. 2010. Defined subunit arrangement and rab interactions are required for functionality of

the HOPS tethering complex. *Traffic*. 11:1334-1346.

Peplowska, K., D.F. Markgraf, C.W. Ostrowicz, G. Bange, and C. Ungermann. 2007. The CORVET tethering complex interacts with the yeast Rab5 homolog Vps21 and is involved in endo-lysosomal biogenesis. *Developmental cell*. 12:739-750.

Perini, E.D., R. Schaefer, M. Stoter, Y. Kalaidzidis, and M. Zerial. 2014. Mammalian CORVET Is Required for Fusion and Conversion of Distinct Early Endosome Subpopulations. *Traffic*. 15:1366-1389.

Pols, M.S., C. ten Brink, P. Gosavi, V. Oorschot, and J. Klumperman. 2013. The HOPS proteins hVps41 and hVps39 are required for homotypic and heterotypic late endosome fusion. *Traffic*. 14:219-232.

Rojo, E., C.S. Gillmor, V. Kovaleva, C.R. Somerville, and N.V. Raikhel. 2001. VACUOLELESS1 is an essential gene required for vacuole formation and morphogenesis in Arabidopsis. *Developmental cell*. 1:303-310.

Rojo, E., J. Zouhar, V. Kovaleva, S. Hong, and N.V. Raikhel. 2003. The AtC-VPS protein complex is localized to the tonoplast and the prevacuolar compartment in arabidopsis. *Molecular biology of the cell*. 14:361-369.

Sakurai, H.T., T. Inoue, A. Nakano, and T. Ueda. 2016. ENDOSOMAL RAB EFFECTOR WITH PX-DOMAIN, an Interacting Partner of RAB5 GTPases, Regulates Membrane Trafficking to Protein Storage Vacuoles in Arabidopsis. *The Plant cell*. 28:1490-1503.

Sato, M.H., N. Nakamura, Y. Ohsumi, H. Kouchi, M. Kondo, I. Hara-Nishimura, M. Nishimura, and Y. Wada. 1997. The AtVAM3 encodes a syntaxin-related molecule implicated in the vacuolar assembly in *Arabidopsis thaliana*. *The Journal of biological chemistry*. 272:24530-24535.

Seals, D.F., G. Eitzen, N. Margolis, W.T. Wickner, and A. Price. 2000. A Ypt/Rab effector complex containing the Sec1 homolog Vps33p is required for homotypic vacuole fusion. *Proceedings of the National Academy of Sciences of the United States of America*. 97:9402-9407.

Singh, M.K., F. Kruger, H. Beckmann, S. Brumm, J.E. Vermeer, T. Munnik, U. Mayer, Y.D. Stierhof, C. Grefen, K. Schumacher, and G. Jurgens. 2014. Protein delivery to vacuole requires SAND protein-dependent Rab GTPase conversion for MVB-vacuole fusion. *Current biology : CB*. 24:1383-1389.

Tan, X., J. Wei, B. Li, M. Wang, and Y. Bao. 2017. AtVps11 is essential for vacuole biogenesis in embryo and participates in pollen tube growth in Arabidopsis. *Biochemical and biophysical research communications*. 491:794-799.

Ueda, T., M. Yamaguchi, H. Uchimiya, and A. Nakano. 2001. Ara6, a plant-unique novel type Rab GTPase, functions in the endocytic pathway of *Arabidopsis thaliana*. *The EMBO journal*. 20:4730-4741.

Viotti, C., J. Bubeck, Y.D. Stierhof, M. Krebs, M. Langhans, W. van den Berg, W. van Dongen, S. Richter, N. Geldner, J. Takano, G. Jurgens, S.C. de Vries, D.G. Robinson, and K. Schumacher. 2010. Endocytic and secretory traffic in Arabidopsis merge in the trans-Golgi network/early endosome, an independent and highly dynamic organelle. *The Plant cell*. 22:1344-1357.

Vukašinović, N., and V. Žárský. 2016. Tethering Complexes in the Arabidopsis Endomembrane System. *Frontiers in Cell and Developmental Biology*. 4.

Wickner, W., and R. Schekman. 2008. Membrane fusion. *Nature structural & molecular biology*. 15:658-664.

Yamaguchi, M., M. Kubo, H. Fukuda, and T. Demura. 2008. Vascular-related NAC-

DOMAIN7 is involved in the differentiation of all types of xylem vessels in Arabidopsis roots and shoots. *The Plant journal : for cell and molecular biology*. 55:652-664.

Zhang, C., G.R. Hicks, and N.V. Raikhel. 2014. Plant vacuole morphology and vacuolar trafficking. *Frontiers in plant science*. 5:476.